Modeling and interpretation of extracellular potentials

Gaute T. Einevoll[1], Szymon Łęski[2], Espen Hagen[1]

[1]*Computational Neuroscience Group (compneuro.umb.no)*
Norw. Univ of Life Sci. (UMB), Ås; Norwegian Node of INCF

[2] *Nencki Institute of Experimental Biology, Warsaw*
Polish Node of INCF

incf International Neuroinformatics Coordinating Facility

nencki institute of experimental biology

Overall plan for tutorial

- 9.00-9.50: Lecture 1 (Gaute)
- 9.50-10.05: Break
- 10.05-10.55: Lecture 2(Gaute & Szymon)
- 10.55-11.10: Break
- 11.10-12.00: Lecture 3 (Szymon)
- 12.00-13.00: Lunch break
- 13.00-: Tutorials (Espen & Szymon)

Physiological measures of neural activity

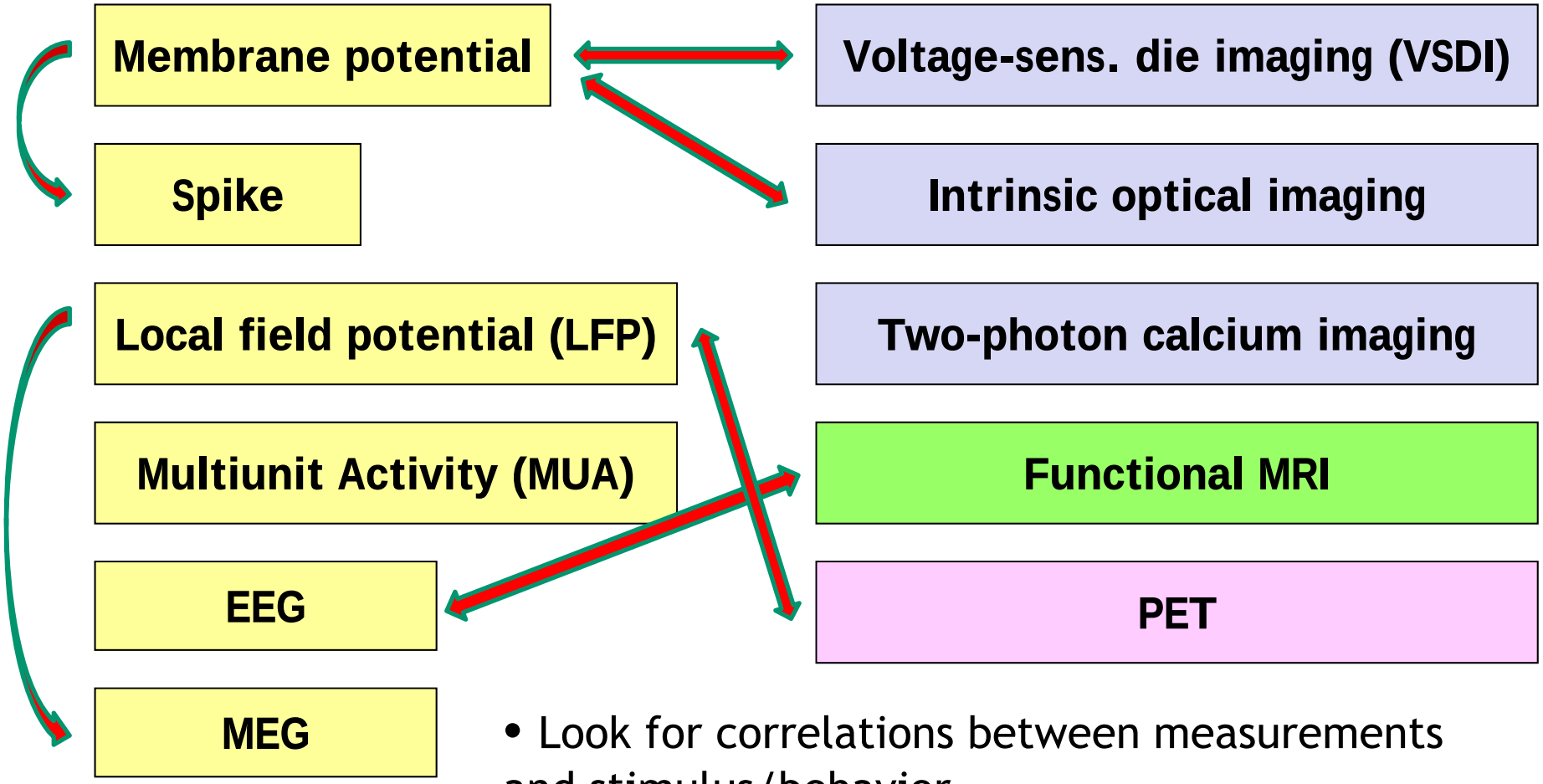

- Look for correlations between measurements and stimulus/behavior

- Typical multimodal analysis: Look for correlations between different experiments

Physics-type multimodal modeling

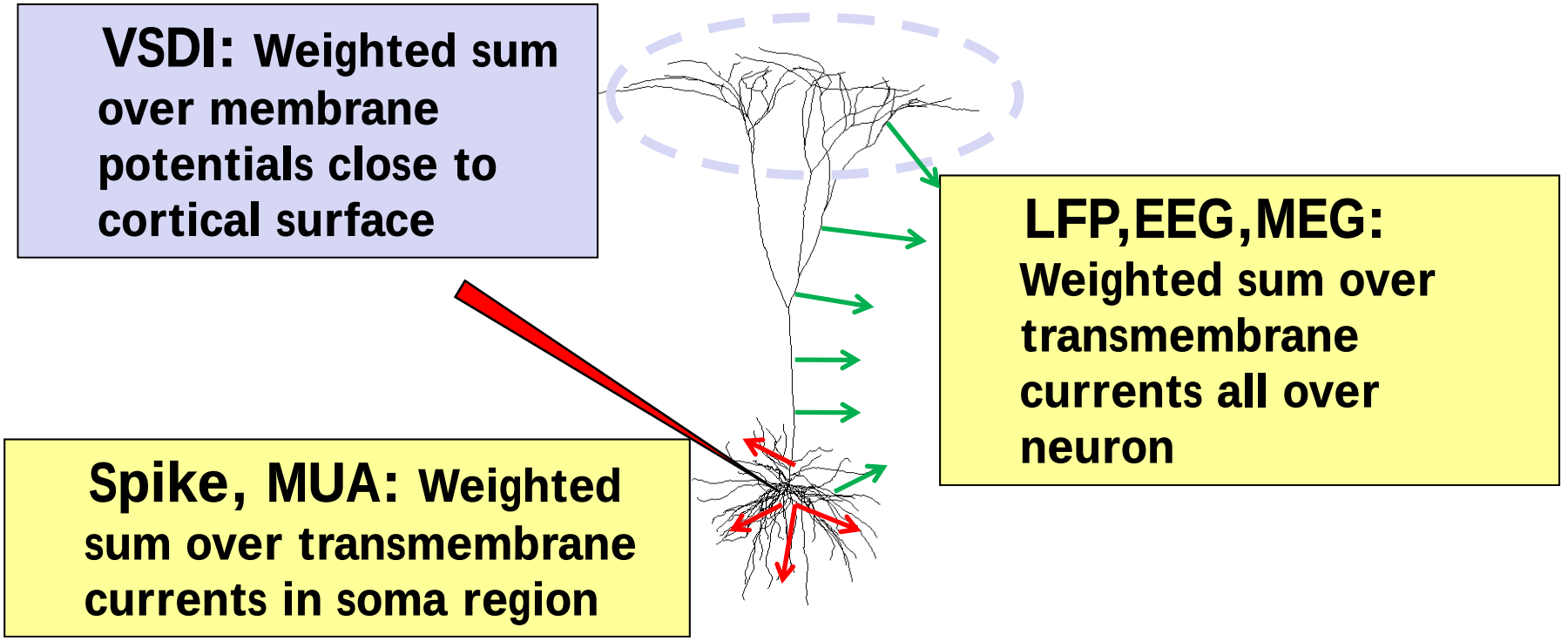

- Need to work out mathematical connections between neuron dynamics and different experimental modalities (”*measurement physics*”)

’Modeling what you can measure’

- A candidate model for, say, network dynamics in a cortical column should predict all available measurement modalities

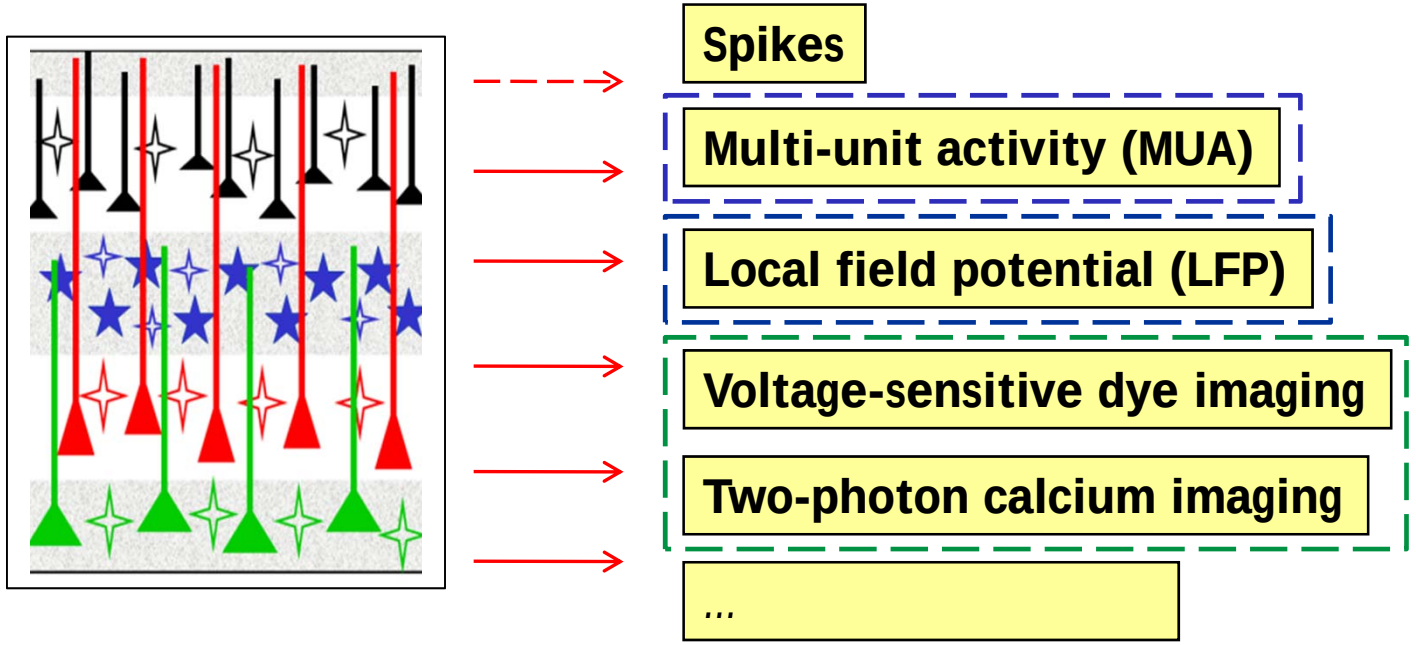

- And we need neuroinformatics tools to make this as simple as possible

Measuring electrical potentials in the brain

- Among the oldest and (conceptually) simplest measurents of neural activity

- Richard Caton (1875): Measures electrical potentials from surfaces of animal brains (ECoG)

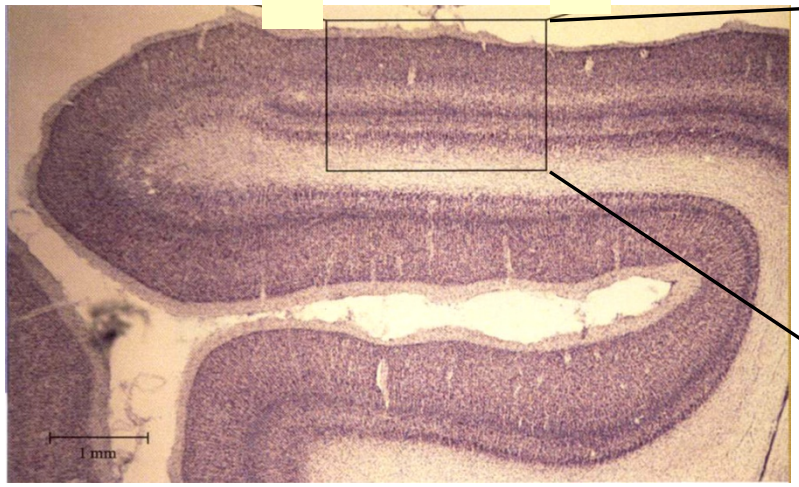

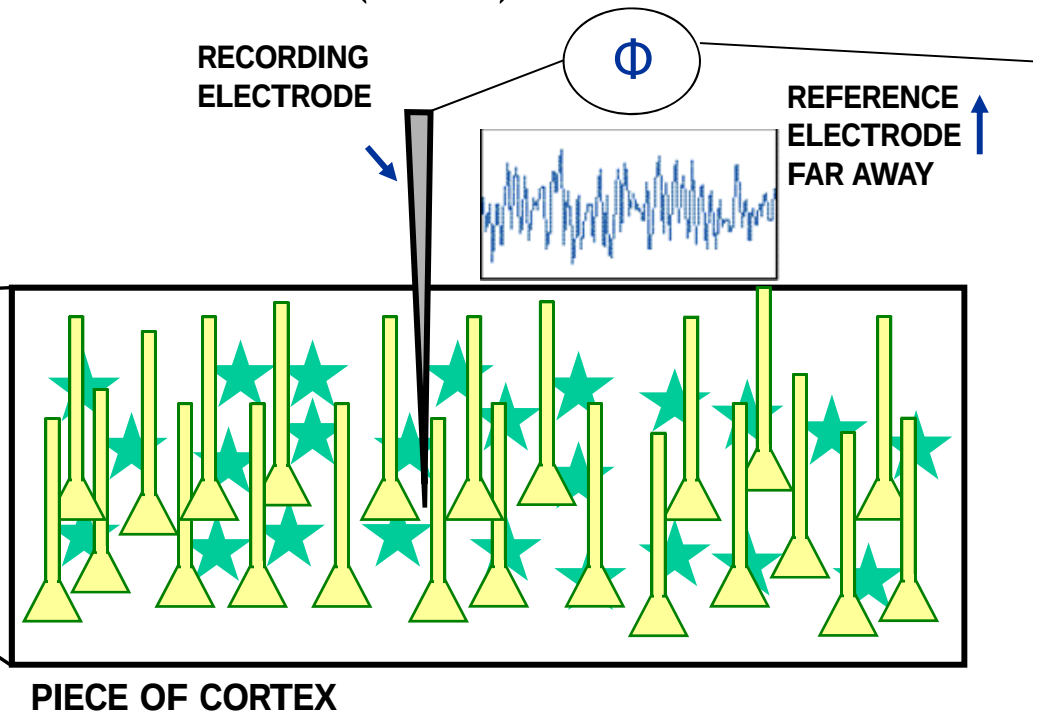

Typical data analysis

- Recorded signal split into two frequency bands:
  - ➢ High-frequency band (>~ 500 Hz): **Multi-unit activity (MUA)**, *measures spikes in neurons surrounding electron tip*
  - ➢ Low-frequency band (<~300 Hz): **Local field potential (LFP),** *measures subthreshold activity*

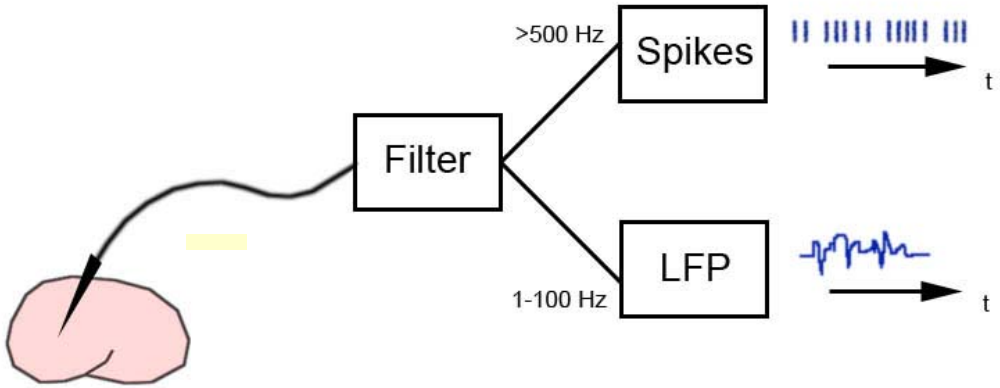

- LFP often discarded
- Sometimes used for current-source density (CSD) analysis with laminar-electrode recordings spanning cortical layers

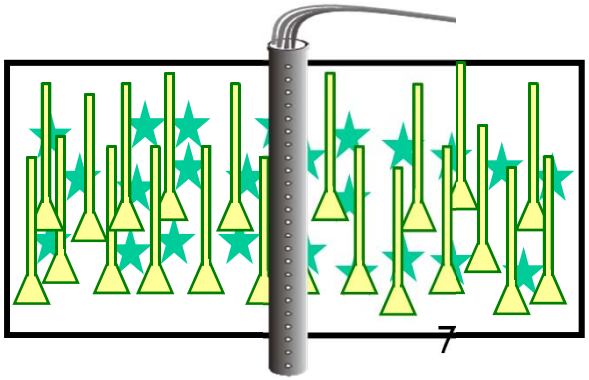

Revival of LFP in last decade

- LFP is unique window into activity in *populations* (thousands) of neurons

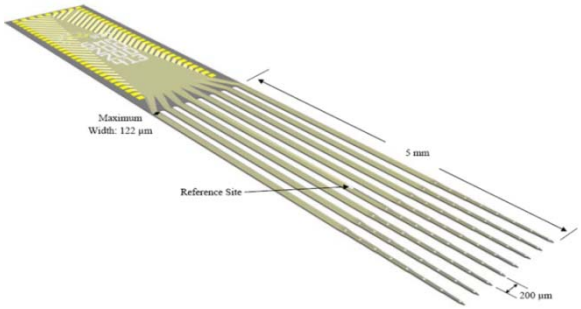

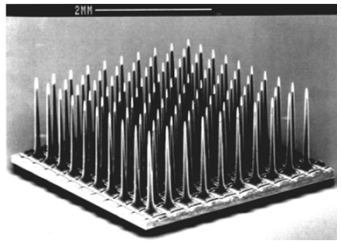

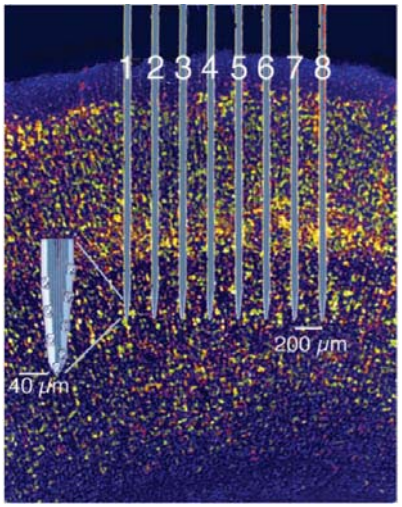

- New generation of silicon-based multielectrodes with up to thousands of contacts offers new possibilities

- Candidate signal for brain-computer interfaces (BCI); more stable than spikes

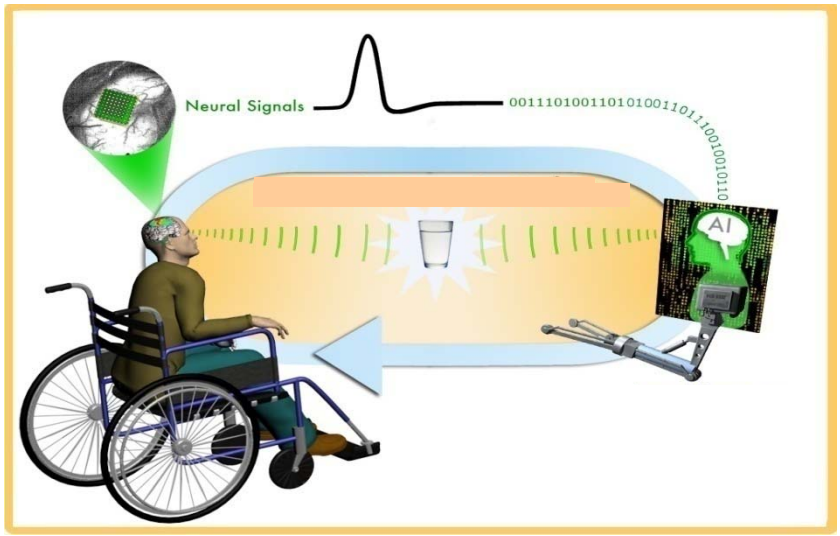

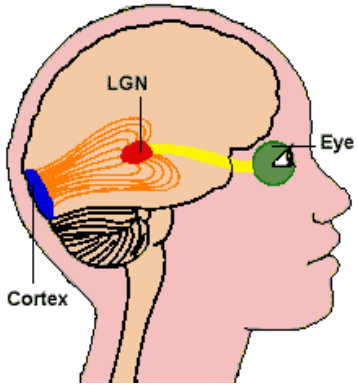

Rat whisker system:
laminar electrode recordings

(Anna Devor, Anders Dale, UC San Diego;
Istvan Ulbert, Hungarian Acad. Sci, Budapest)

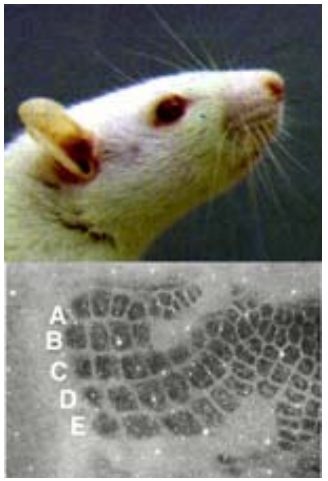

"V1" ← **Barrel cortex** →

"LGN" ← **Thalamus (VPM)** →

"RETINA" ← **Brainstem** →

"EYE" ← **Whisker** →

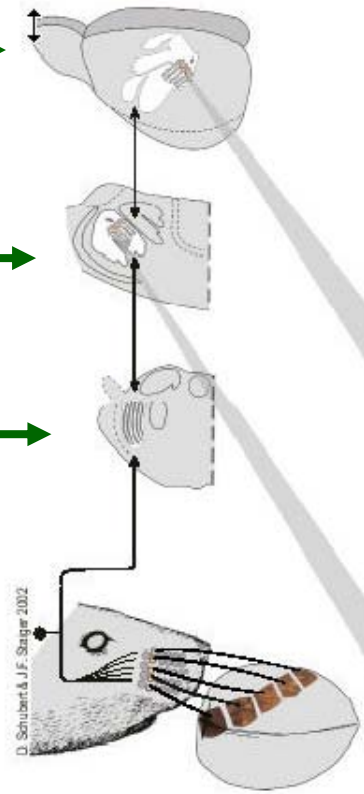

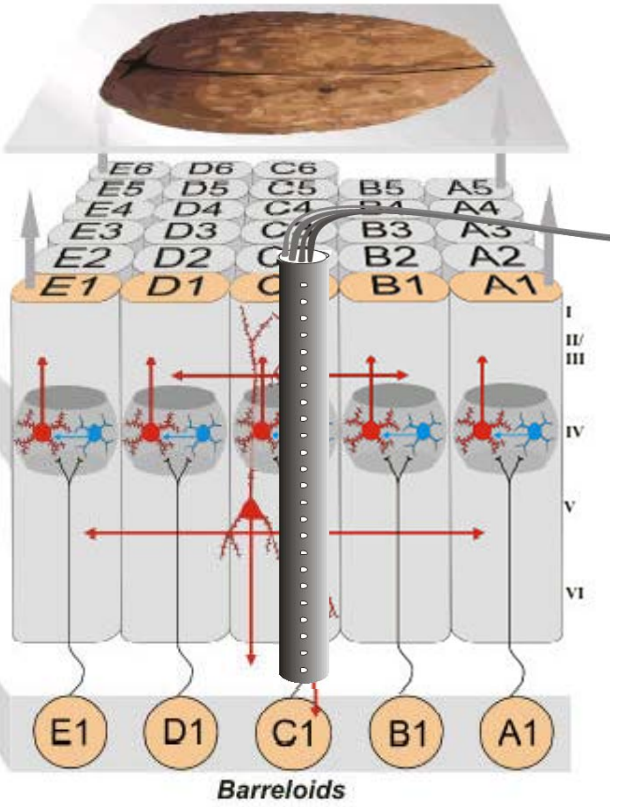

Laminar electrode recordings from rat barrel cortex – single whisker flick

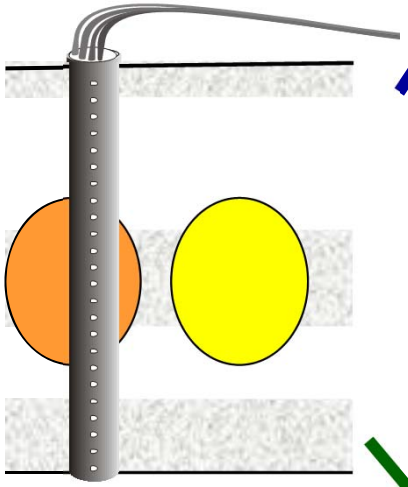

Low-pass filter (<500 Hz): **LOCAL FIELD POTENTIAL (LFP)**

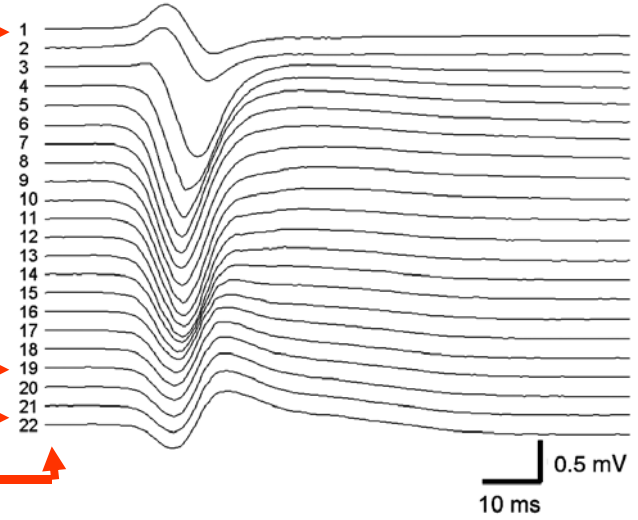

Measure of **dendritic processing** of synaptic input?

High-pass filter (>750Hz), rectification : **MULTI-UNIT ACTIVITY (MUA)**

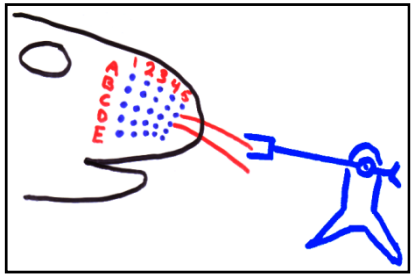

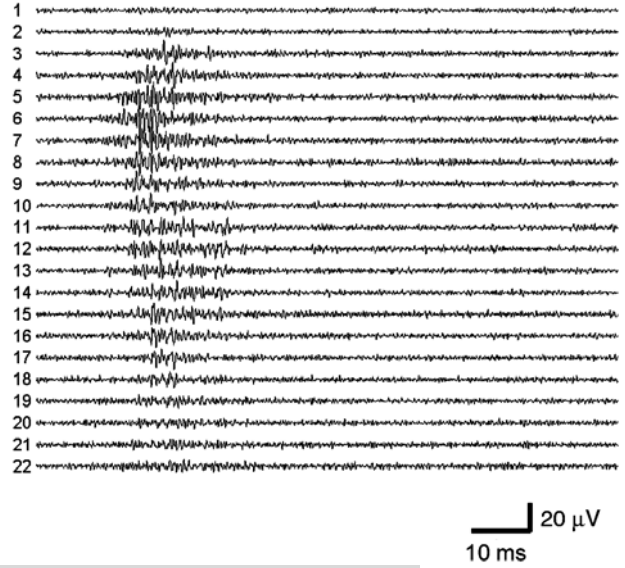

Measure of neuronal **action potentials?**

Einevoll et al, J Neurophysiol 2007

Physical origin of LFP and MUA

- Source of extracellular potential: *Transmembrane* currents

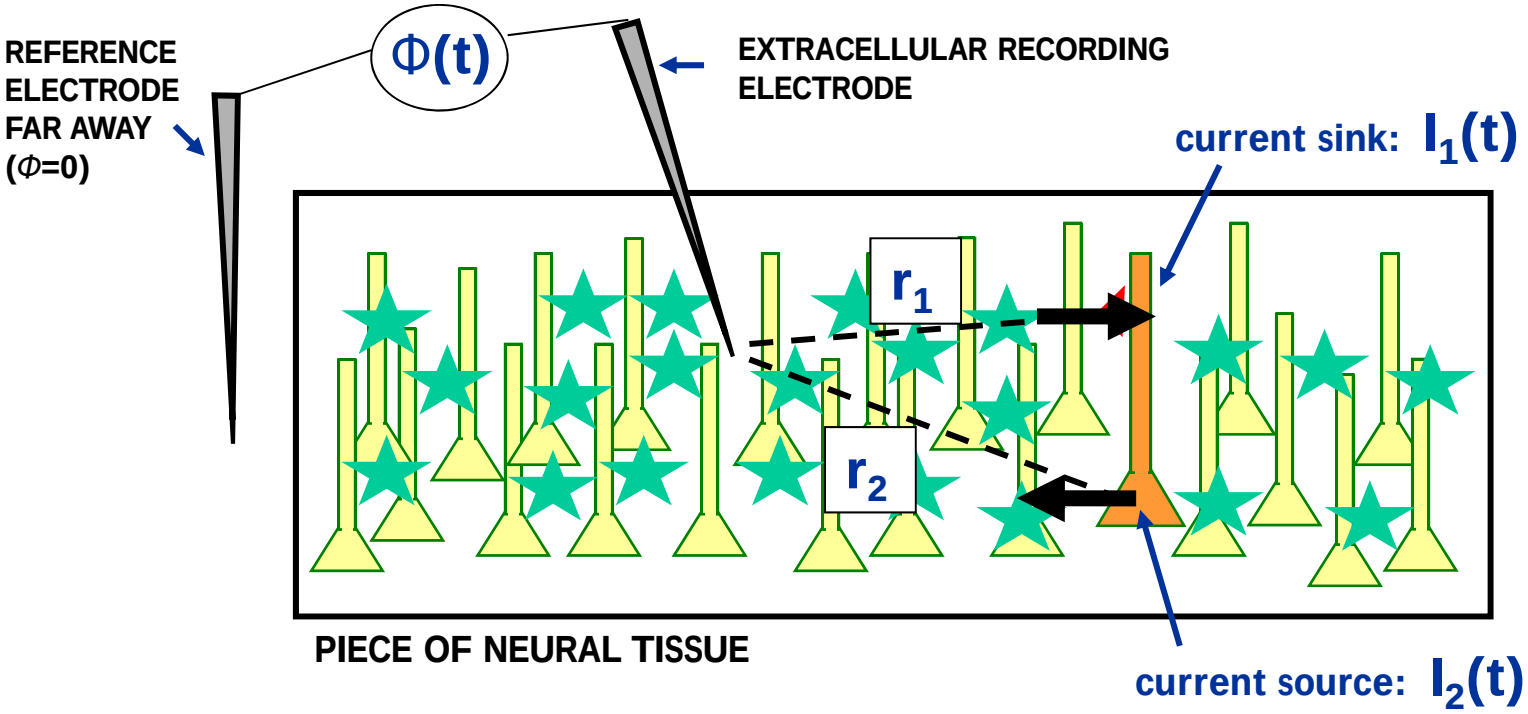

FORWARD SOLUTION: $$\phi(t) = \frac{I_1(t)}{4\pi\sigma r_1} + \frac{I_2(t)}{4\pi\sigma r_2}$$

σ: extracellular conductivity

Note: Current monopoles do not exist

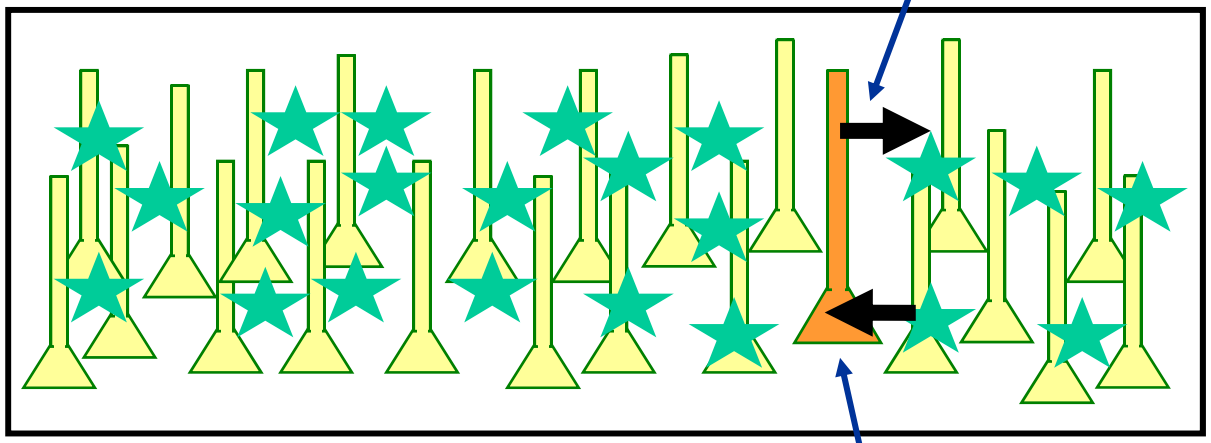

$$\phi(t) = \frac{I_1(t)}{4\pi\sigma r_1} + \frac{I_2(t)}{4\pi\sigma r_2}$$

- Conservation of electric charge requires (capacitive currents included!):

$$I_1(t) + I_2(t) = 0$$

$$\phi(t) = \frac{I(t)}{4\pi\sigma r_1} - \frac{I(t)}{4\pi\sigma r_2}$$

- From far away it looks like a **current dipole**

Assumptions underlying:

$$\phi(t) = \frac{I(t)}{4\pi\sigma r_1} - \frac{I(t)}{4\pi\sigma r_2}$$

I. Quasistatic approximation to Maxwell's equations

$$\nabla \cdot \mathbf{E} = \frac{\rho}{\epsilon_0}$$

$$\nabla \cdot \mathbf{B} = 0$$

$$\nabla \times \mathbf{E} = -\frac{\partial \mathbf{B}}{\partial t}$$

$$\nabla \times \mathbf{B} = \mu_0 \mathbf{j} + \frac{1}{c^2}\frac{\partial \mathbf{E}}{\partial t}$$

- sufficiently low frequencies so that electrical and magnetic fields are decoupled (OK for f ≪ 10 kHz)

- here: not interested in magnetic fields

- then:

$$\nabla \times \mathbf{E} = 0 \quad \Rightarrow \quad \mathbf{E} = -\nabla\phi$$

Assumptions underlying:

$$\phi(t) = \frac{I(t)}{4\pi\sigma r_1} - \frac{I(t)}{4\pi\sigma r_2}$$

II. Coarse-grained extracellular medium described by **extracellular conductivity σ**

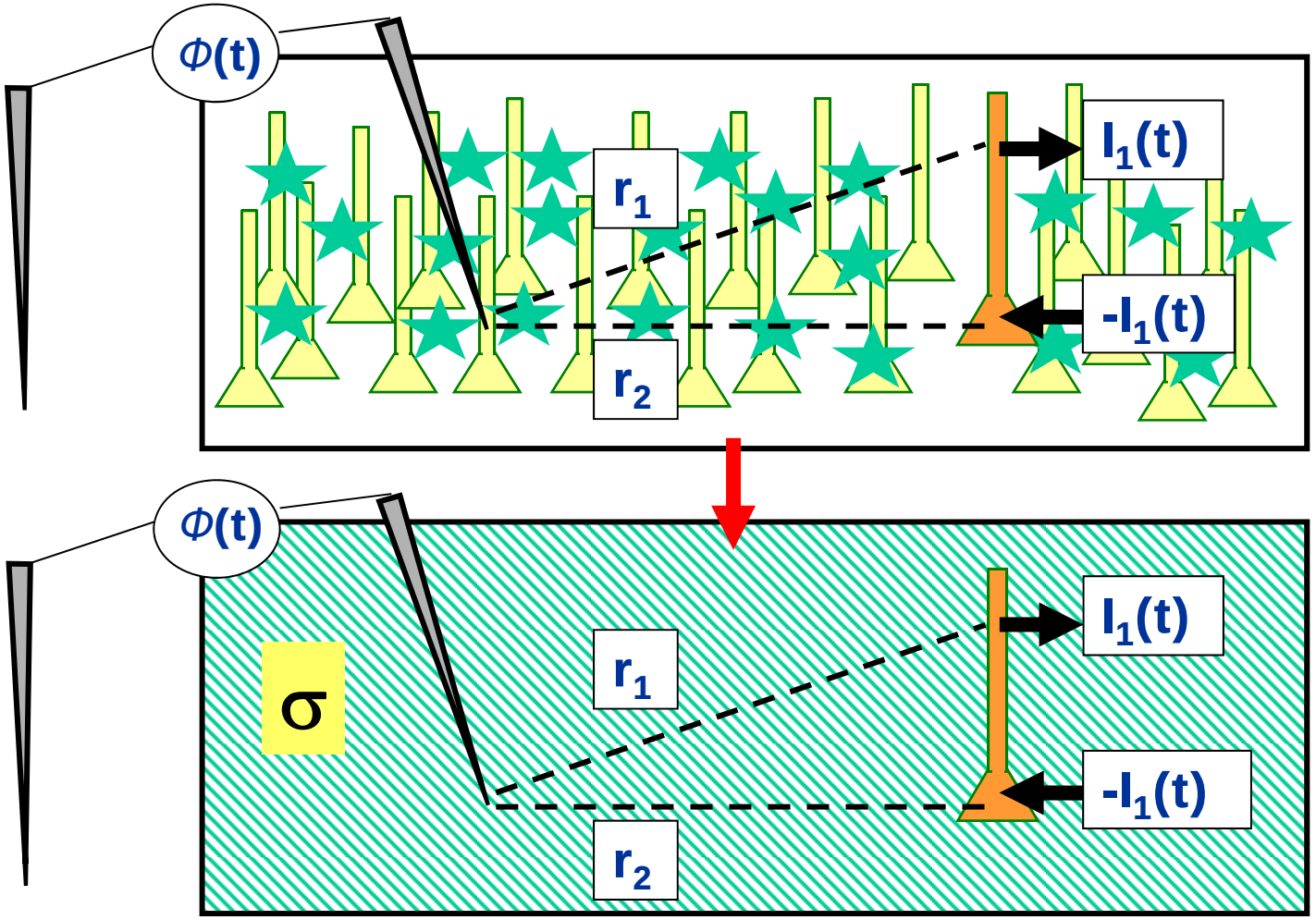

Assumptions underlying:

$$\phi(t) = \frac{I(t)}{4\pi\sigma r_1} - \frac{I(t)}{4\pi\sigma r_2}$$

III. **Linear** extracellular medium

$$\mathbf{j} = \sigma \mathbf{E}$$

j: current density (A/m^2**)**

E: electric field (V/m**)**

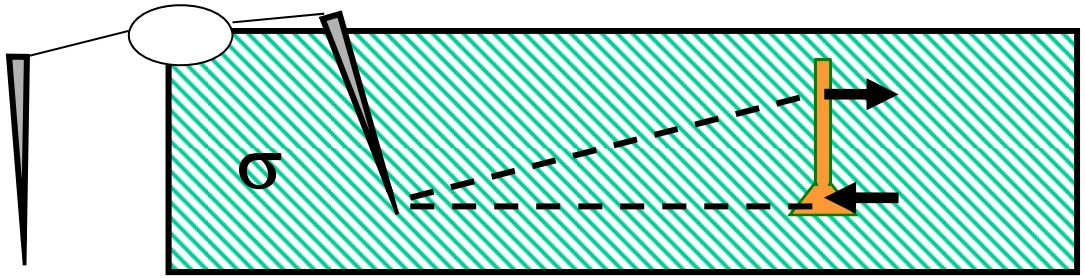

IV. Extracellular medium is

1. **Ohmic**
2. **homogeneous**
3. **frequency-independent**
4. **isotropic**

Assumptions underlying:

$$\phi(t) = \frac{I(t)}{4\pi\sigma r_1} - \frac{I(t)}{4\pi\sigma r_2}$$

IV.1: Ohmic: σ is real, that is, extracellular medium is not capacitive

- **OK**

IV.2: Homogeneous: σ is the same at all positions

- **OK** inside cortex, but lower σ in white matter
- Formula can be modified my means of «method of images» from electrostatics

IV. 3: Frequency-independent: σ is same for all frequencies

- Probably **OK** (I think), but still somewhat debated
- But if frequency dependence is found, formalism can easily be adapted

Assumptions underlying:

$$\phi(t) = \frac{I(t)}{4\pi\sigma r_1} - \frac{I(t)}{4\pi\sigma r_2}$$

IV.4 Isotropic: σ is the same in all directions

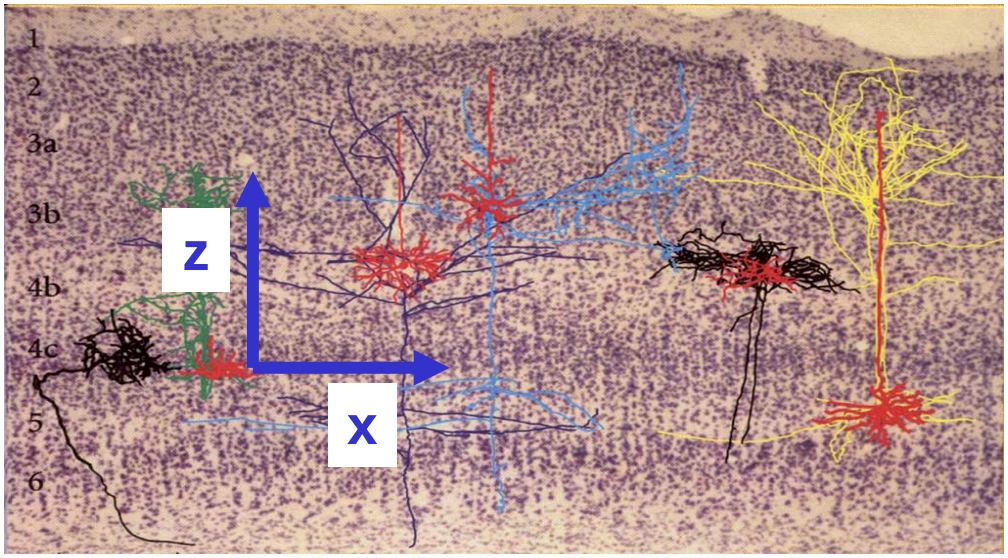

- σ is in general a tensor $(\sigma_x, \sigma_y, \sigma_z)$

- Easier to move along apical dendrites than across ($\sigma_z > \sigma_x$ and σ_y)

- Cortex: $\sigma_z \sim 1\text{-}1.5\ \sigma_{x,y}$

- Generalized formula:

$$\phi(t) = \frac{I(t)}{4\pi\sqrt{\sigma_y\sigma_z x_1^2 + \sigma_z\sigma_x y_1^2 + \sigma_x\sigma_y z_1^2}} - \frac{I(t)}{4\pi\sqrt{\sigma_y\sigma_z x_2^2 + \sigma_z\sigma_x y_2^2 + \sigma_x\sigma_y z_2^2}}$$

Forward-modeling formula for multicompartment neuron model

$$\phi(\mathbf{r},t) = \frac{1}{4\pi\sigma}\sum_{n=1}^{N}\frac{I_n(t)}{|\mathbf{r}-\mathbf{r}_n|}$$

Current conservation:

$$\sum_{n=1}^{N} I_n(t) = 0$$

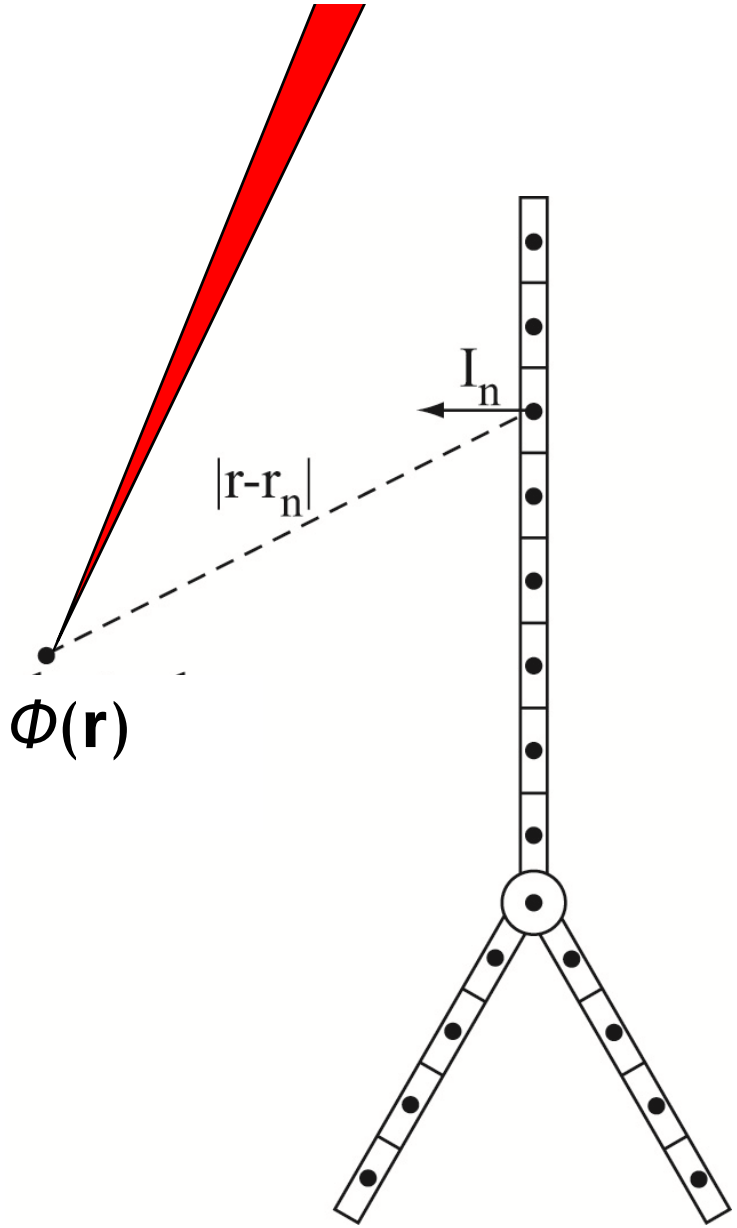

Inverse electrostatic solution

- No charge pileup in extracellular medium:

transmembrane currents

$$\nabla \cdot \mathbf{j}_{tot} = \nabla \cdot (\sigma \mathbf{E} + \mathbf{j}_s) = 0$$

$$\mathbf{E} = -\nabla \phi$$

$$\nabla^2 \phi = -\nabla \cdot \mathbf{E} = \frac{1}{\sigma} \nabla \cdot \mathbf{j}_s$$

- Inverse solution:

$$\nabla^2 \phi = -\frac{1}{\sigma} \sum_{n=1}^{N} I_n(t) \delta^3(\mathbf{r} - \mathbf{r}_n)$$

- Forward solution:

$$\phi(\mathbf{r}, t) = \frac{1}{4\pi\sigma} \sum_{n=1}^{N} \frac{I_n(t)}{|\mathbf{r} - \mathbf{r}_n|}$$

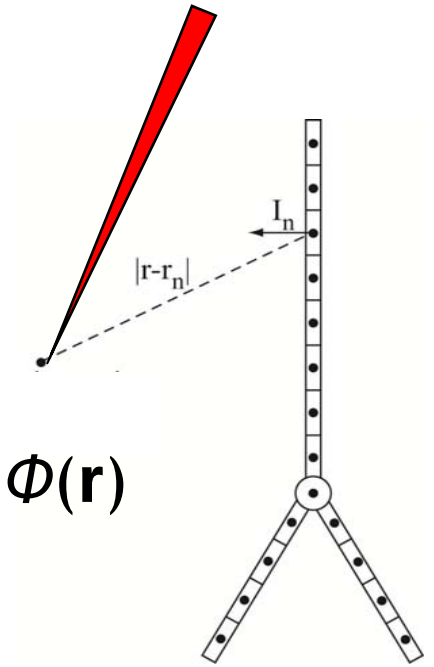

Current source density

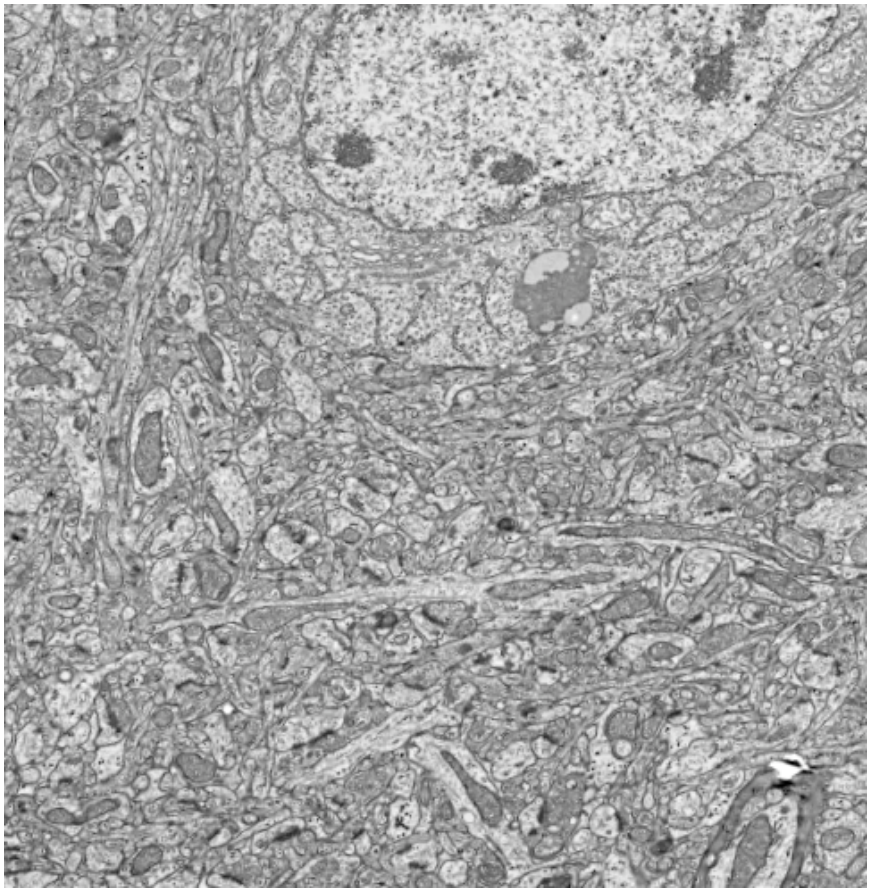

- Neural tissue is a spaghetti-like mix of dendrites, axons, glial branches at micrometer scale

- In general, the extracellular potential will get contributions from a mix of all these

- **Current source density** (CSD) [$C(x,y,z)$]: density of current leaving (sink) or entering (source) extracellular medium in a volume, say, 10 micrometers across [A/m^3]

Electrostatic solution for CSD

$$\nabla^2\phi = -\nabla\cdot\mathbf{E} = \frac{1}{\sigma}\nabla\cdot\mathbf{j}_s$$

- Definition of CSD: $C \equiv -\nabla\cdot\mathbf{j}_s$

- Inverse solution: $\nabla^2\phi(x,y,z) = -\frac{1}{\sigma}C(x,y,z)$

- Forward solution: $\phi(x,y,z) = \frac{1}{4\pi\sigma}\iiint_{V'}\frac{C(x',y',z')}{\sqrt{(x-x')^2+(y-y')^2+(z-z')^2}}dx'dy'dz'$

Generalization to cases with **position**- and **direction**-dependent σ

- Generalized Poisson equation:

$$\nabla\Big(\sigma(\mathbf{r})\nabla\phi(\mathbf{r},t)\Big) = -C(\mathbf{r},t)$$

- Can always be solved with Finite Element Modeling (FEM)
- Example use: Modeling of MEA experiments (slice, cultures)

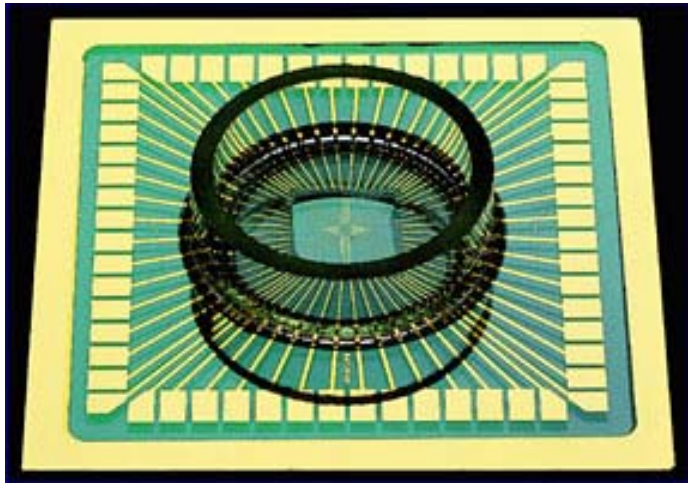

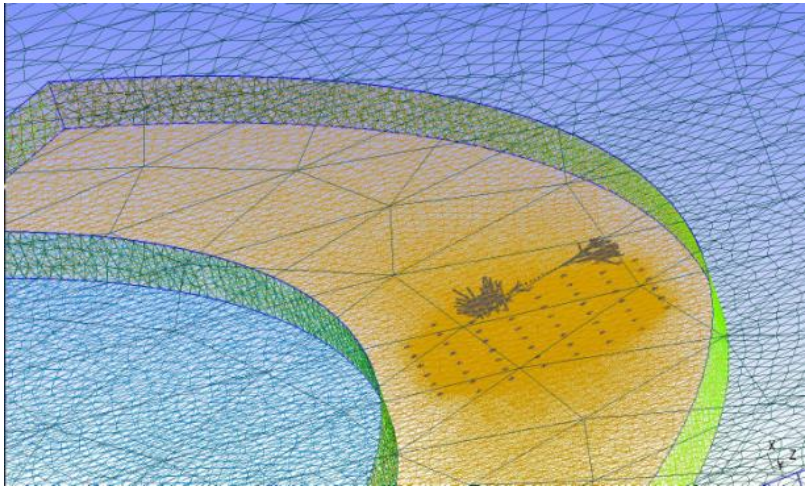

New book

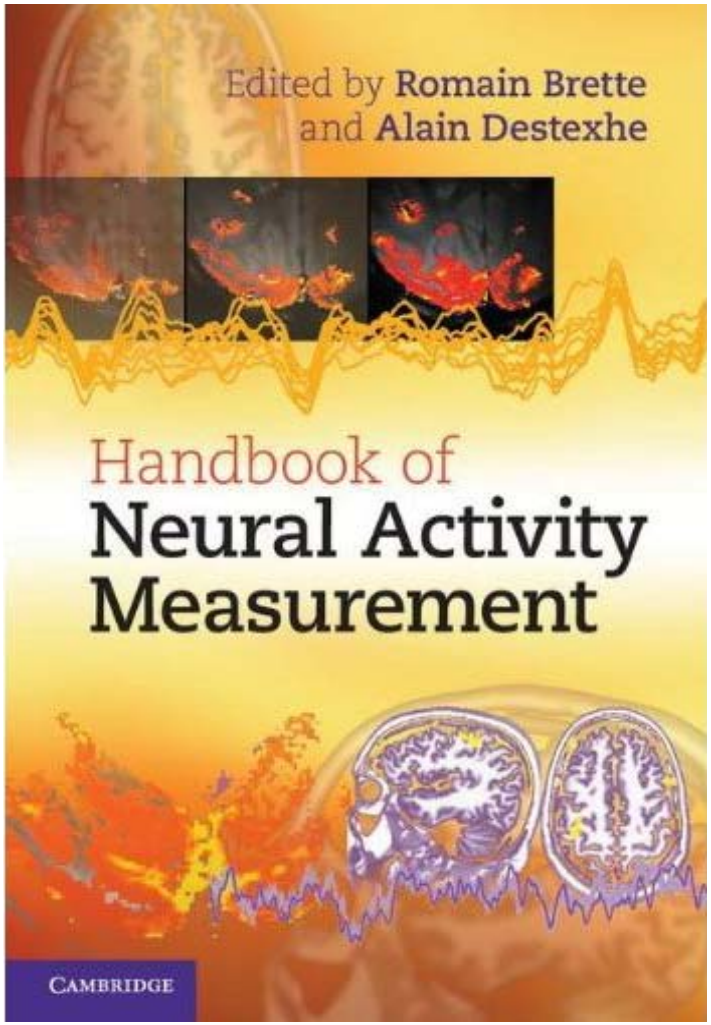

- Chapter on modeling of extracellular potentials:

4

Extracellular spikes and CSD

KLAS H. PETTERSEN, HENRIK LINDÉN, ANDERS M. DALE AND GAUTE T. EINEVOLL

4.1 Introduction

Extracellular recordings have been, and still are, the main workhorse when measuring neural activity in vivo. In single-unit recordings sharp electrodes are positioned close to a neuronal soma, and the firing rate of this particular neuron is measured by counting *spikes*, that is, the standardized extracellular signatures of action potentials (Gold et al., 2006). For such recordings the interpretation of the measurements is straightforward, but complications arise when more than one neuron contributes to the recorded extracellular potential. For example, if two firing neurons of the same type are at about the same distance from their somas to the tip of the recording electrode, it may be very difficult to sort the spikes according to from which neuron they originate.

The use of two (*stereotrode* (McNaughton et al., 1983)), four (*tetrode* (Recce and O'Keefe, 1989; Wilson and McNaughton, 1993; Gray et al., 1995; Jog et al., 2002)) or more (Buzsáki, 2004) close-neighbored recording sites allows for improved

Forward-modeling formula for multicompartment neuron model

$$\phi(\mathbf{r},t) = \frac{1}{4\pi\sigma}\sum_{n=1}^{N}\frac{I_n(t)}{|\mathbf{r}-\mathbf{r}_n|}$$

Current conservation:

$$\sum_{n=1}^{N} I_n(t) = 0$$

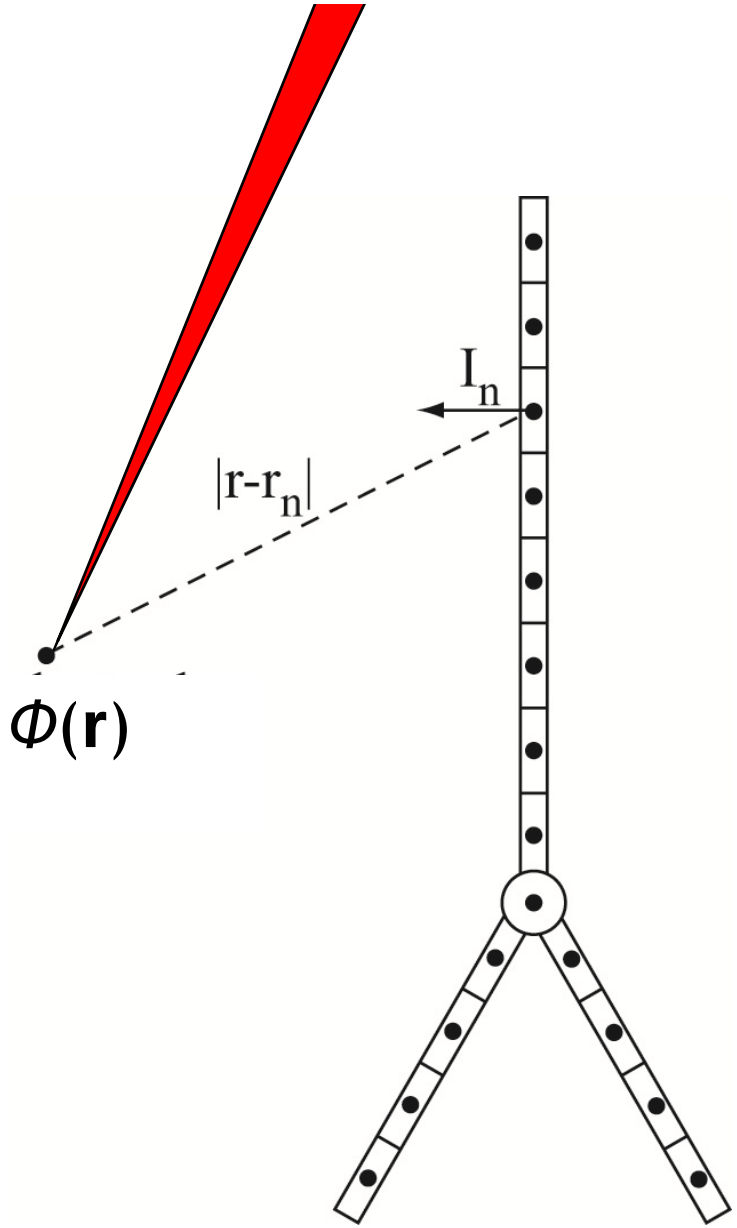

Multicompartmental modeling scheme

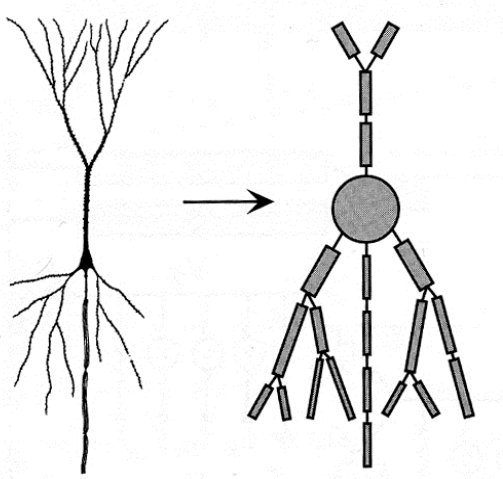

- Example dendritic segment [non-branching case]:

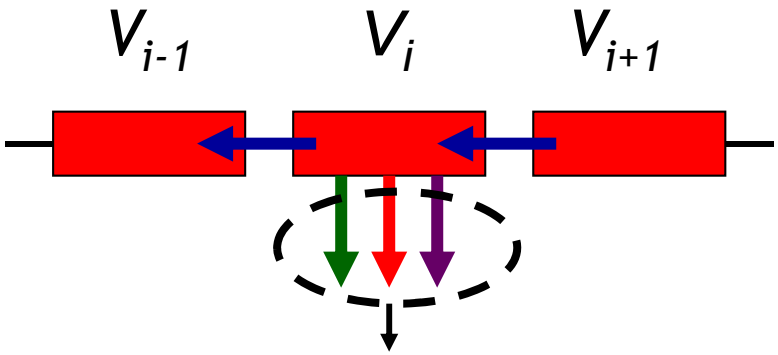

- Kirchhoff's current law ("currents sum to zero"):

transmembrane current

$$g_{i,i+1}(V_{i+1}-V_i)-g_{i-1,i}(V_i-V_{i-1}) = c_i\frac{dV_i}{dt}+g_i^m(V_i-V_r)+\sum_j I_i^j+\sum_s I_i^s$$

CURRENTS TO NEIGHBOURING SEGMENTS

PASSIVE MEMBRANE CURRENT

ACTIVE MEMBRANE CURRENTS

SYNAPTIC CURRENTS

Forward modelling of spikes

What does an **action potential** look like as seen by an extracellular electrode?

[neuron model from
Mainen & Sejnowski, 1996]

From Henze et al (2000):

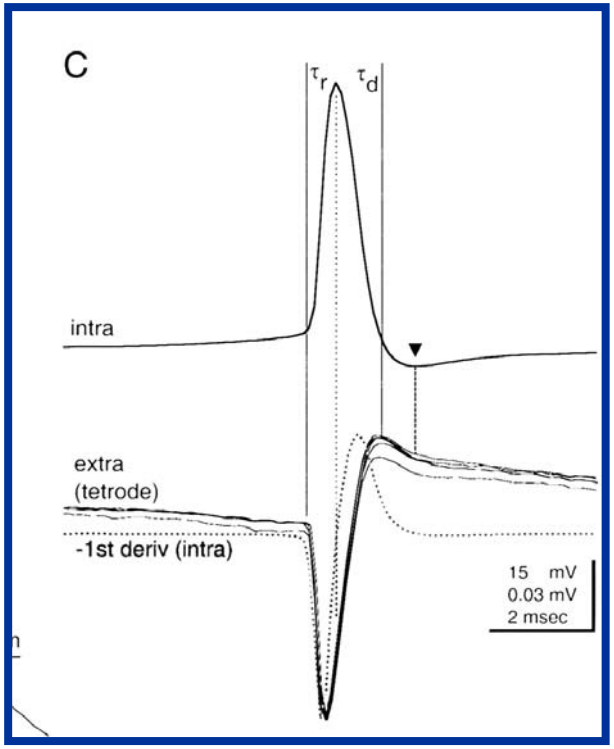

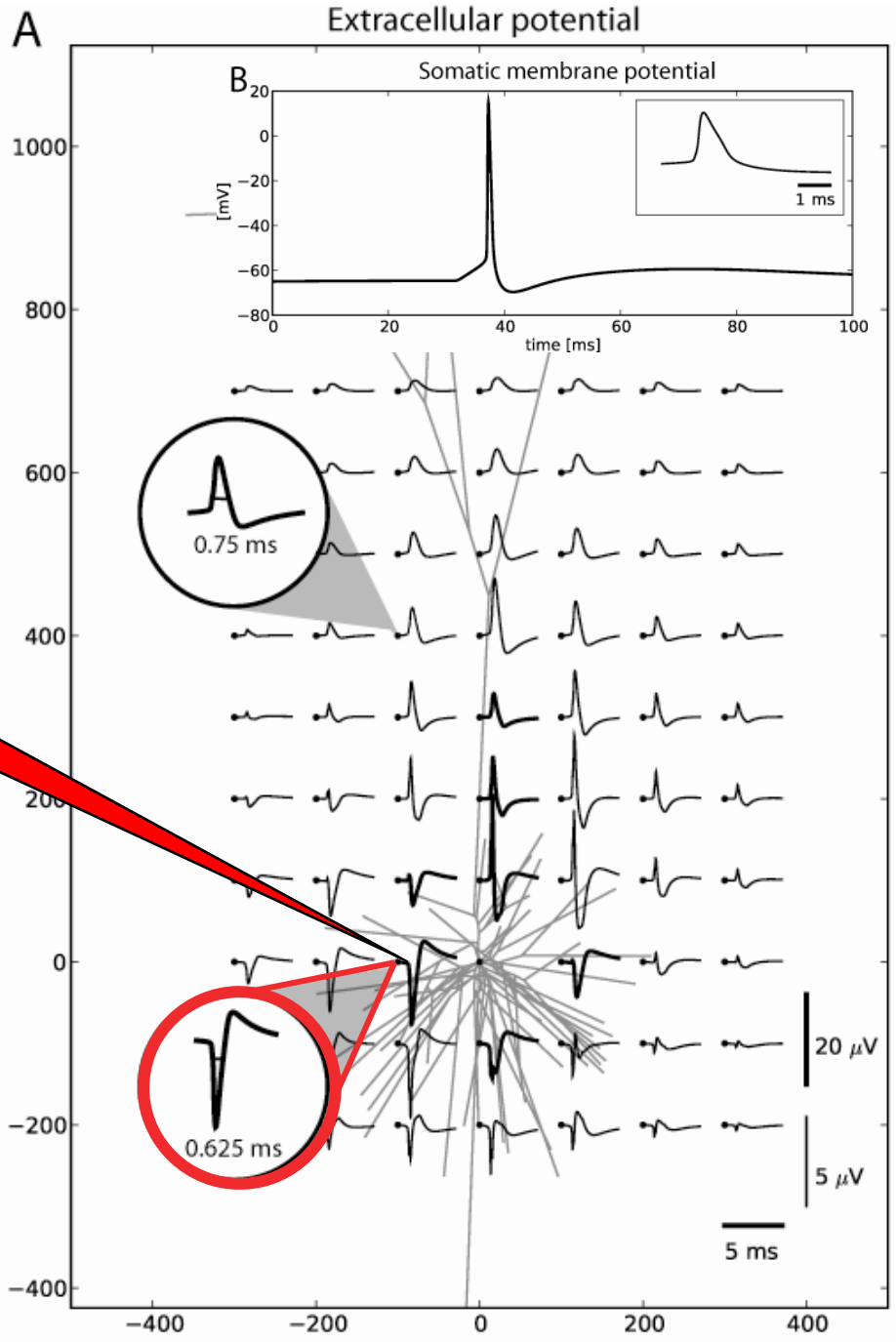

How does the extracellular signature of action potentials depend on neuronal morphology?

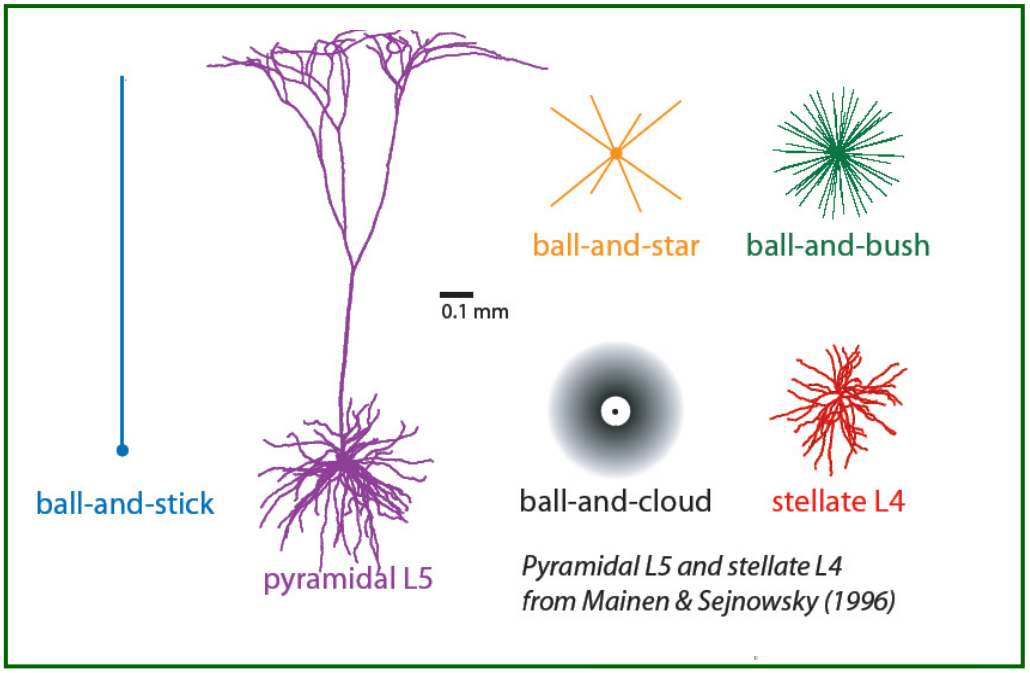

- **Amplitude** is (i) roughly proportional to *sum of cross-sectional areas* of dendrites connected to soma, (ii) independent of *membrane resistance* $R_{m,}$ …

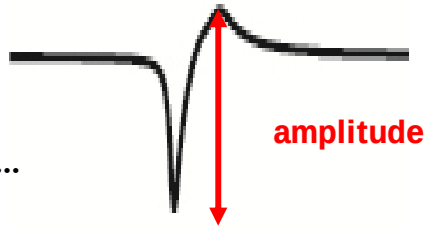

- **Spike width** increases with distance from soma, i.e., high-frequency dampening also with simple ohmic extracellular medium

Pettersen & Einevoll, Biophysical Journal 2008

Spike sorting problem

- Electrodes pick up signals from many spiking neurons; must be sorted

- At present spike so
  - o labor intensive
  - o unreliable

- Need automated sp sorting methods whic
  - o accurate
  - o reproducible
  - o reliable
  - o validated
  - o fast

to take advantage of generation of multiel

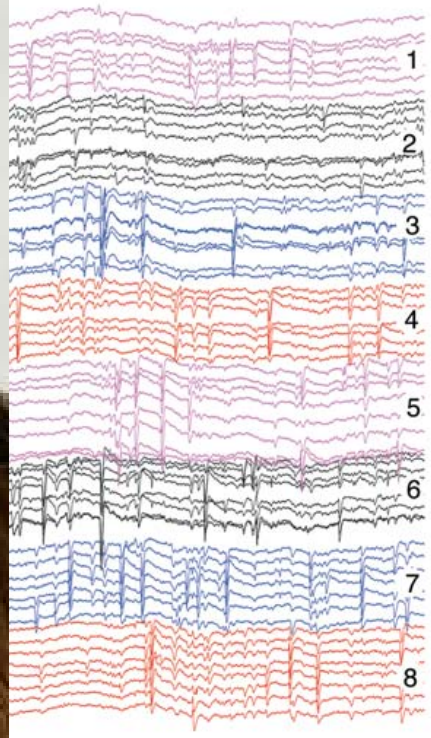

[from Buzsaki, Nature Neurosci, 2004]

Steps in spike sorting

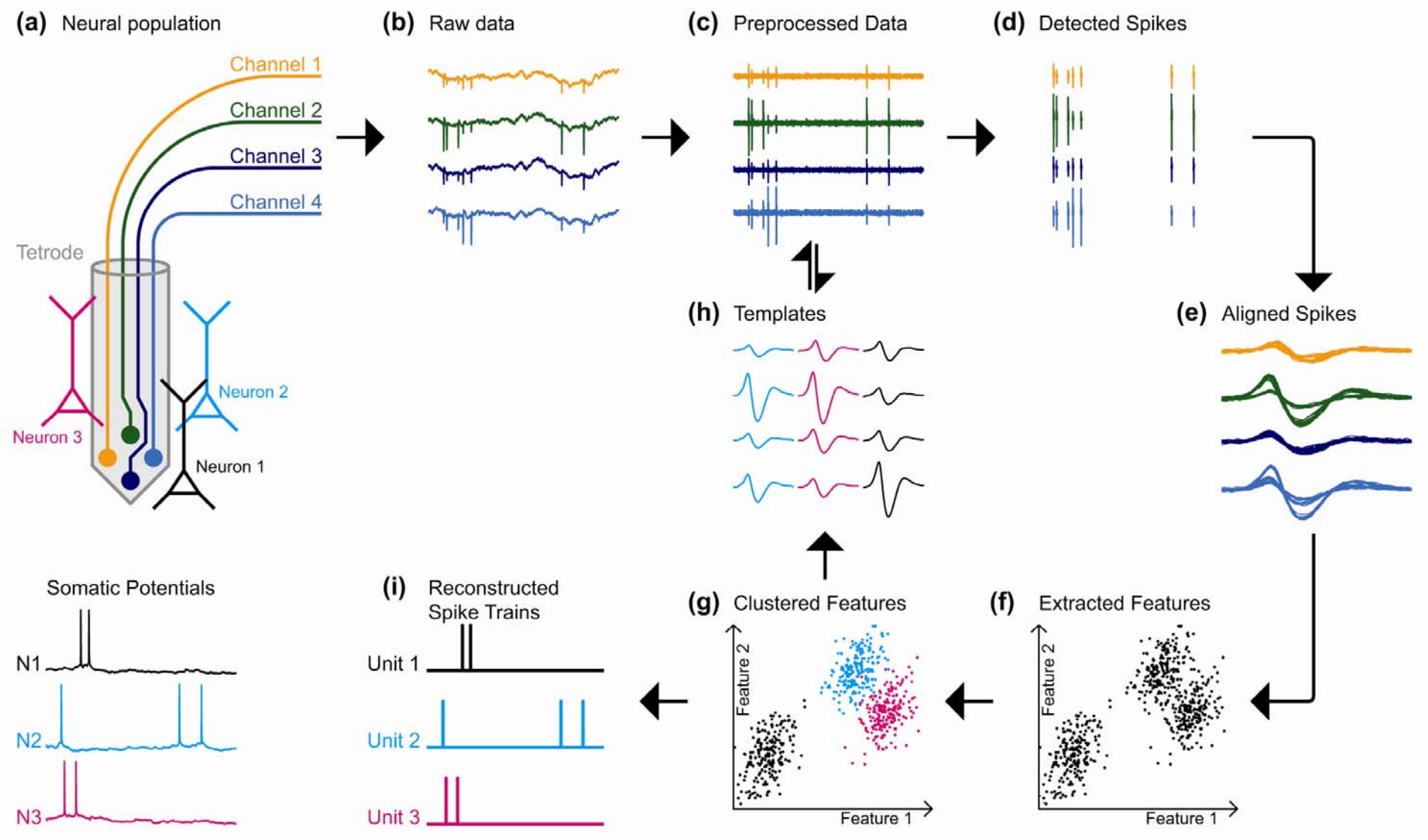

Einevoll et al, Current Opinion Neurobiology 2012

Test data for spike-sorting algorithms

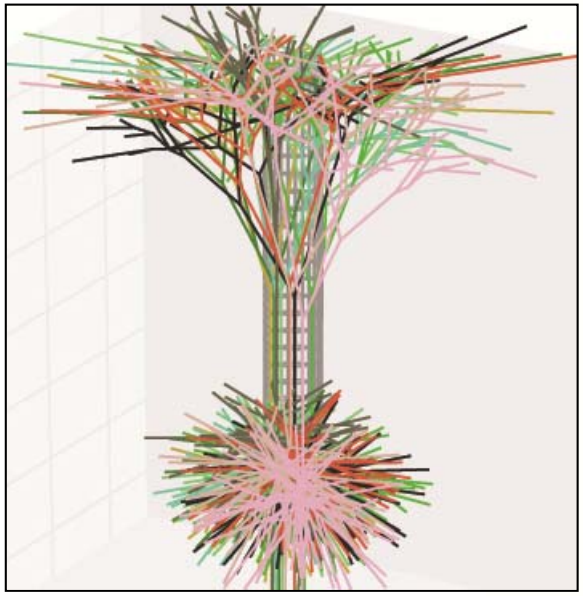

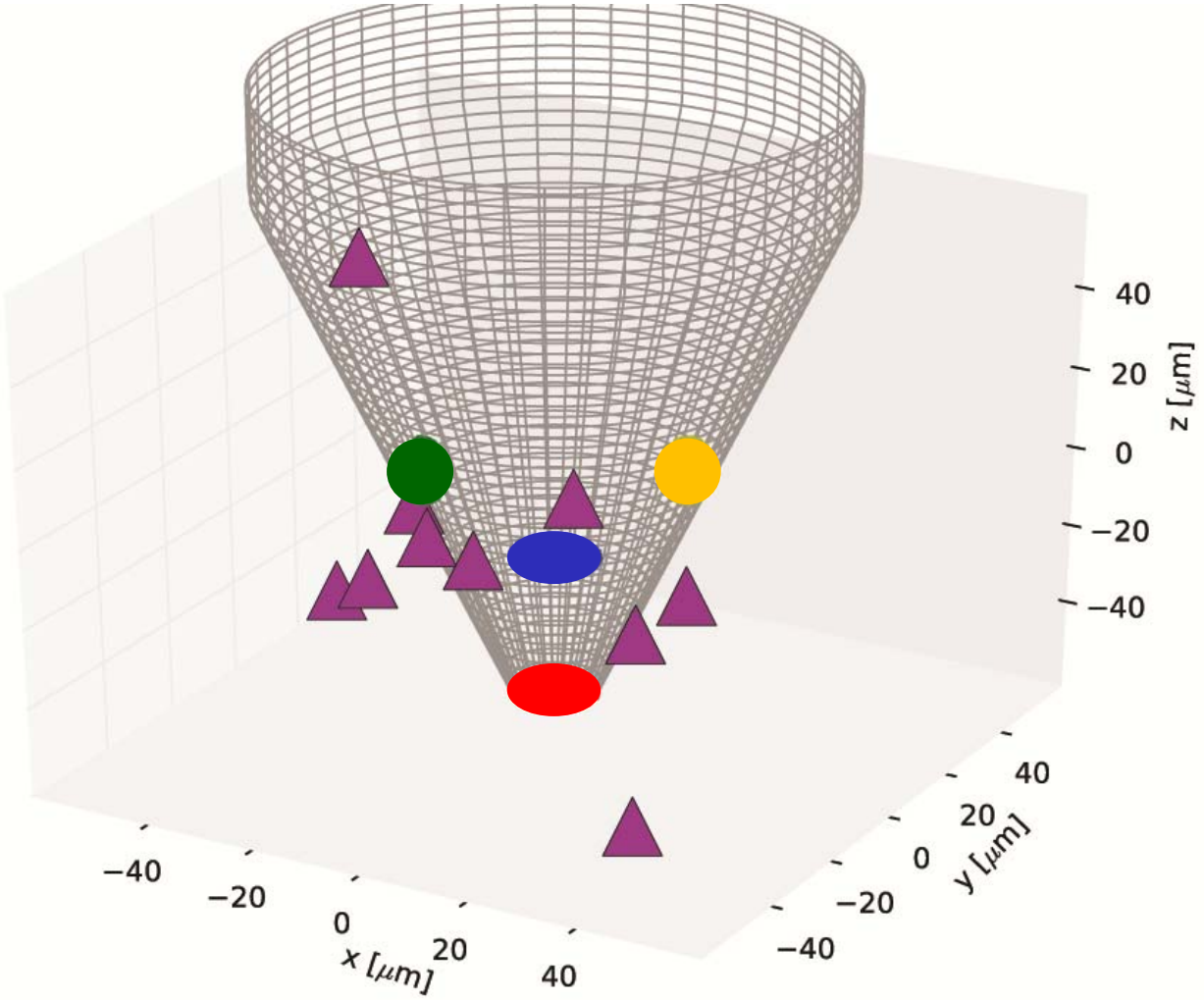

Example model test data

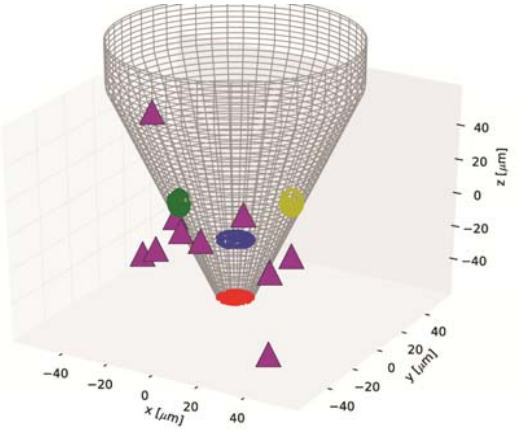

SPIKE SORTING

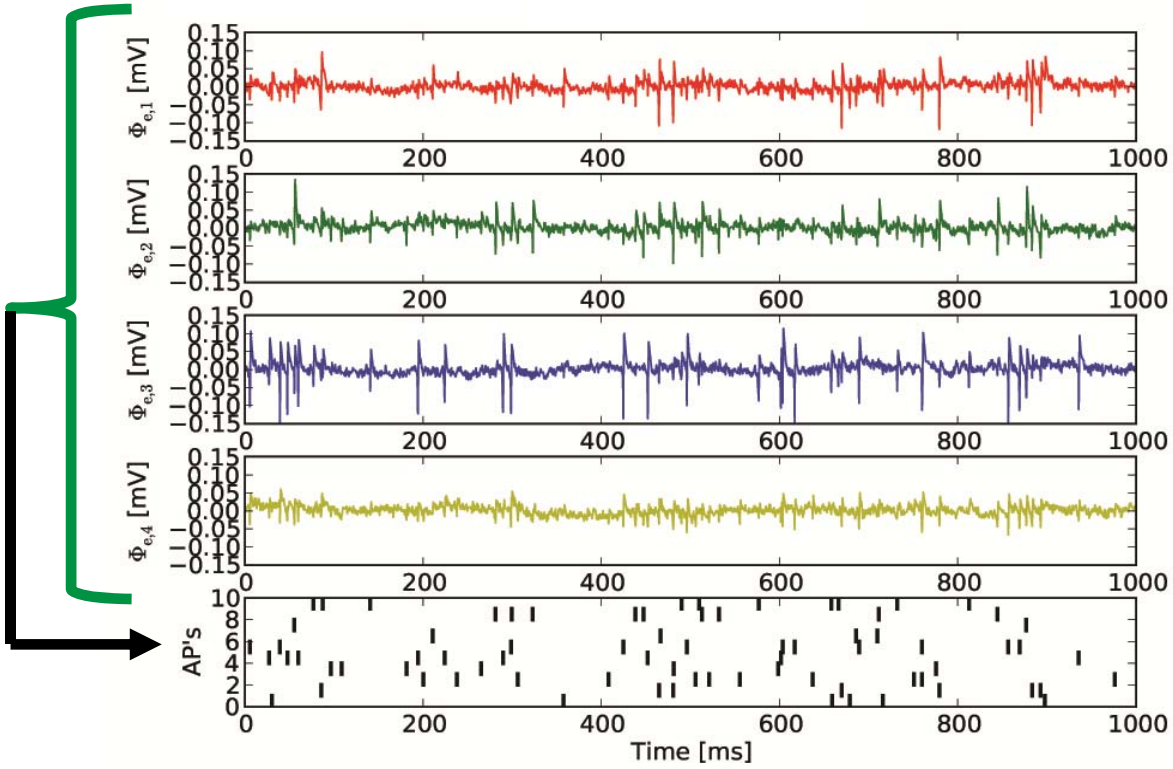

- Can make test data of abitrary complexity by, for example,
  - **(i) varying dendritic morphologies**
  - **(ii) vary spike shapes**
  - **(iii) include adapting or bursting neurons**
  - **(iv) add arbitrary recorded or modeled noise**
  - **(v) tailor correlations in spike times across neurons**

• Collaborative effort on **development** and **validation** of suitable automatic spike-sorting algoritms needed

• Collaborate website shosted by **G-node**, the German node of the International Neuroinformatics Coordinating Facility (INCF)

incf International Neuroinformatics Coordinating Facility

http://www.g-node.org/spike

- **Poster on Tuesday: P143**

Modeling realistic extracellular spiking activity for the purpose of testing automated spike-sorting algorithms

Contact: espen.hagen@umb.no

Espen Hagen[1], Amir Khosrowshahi[1,2], Torbjørn B. Ness[1], Felix Franke[3], Gaute T. Einevoll[1]

[1]Dept. of Mathematical Sciences and Technology, Norwegian University of Life Sciences (UMB), Ås, Norway. [2]Redwood Center for Theoretical Neuroscience, University of California, Berkeley, USA. [3]Bio Engineering Laboratory, ETH Zürich, Basel, Switzerland.

Background

- The basic problem of spike sorting is to infer the activity of individual neuronal sources from extracellular recordings using:
  - point electrodes
  - tetrodes, polytrodes
  - multi-electrode arrays (MEA)
- Traditional spike sorting involve a large manual component
- Manual spike sorting of multichannel recordings is not feasible with the associated data amounts recorded by new generations of recording devices
- But, validation of automated spike-sorting methods are needed, as discussed in a recent review[1].

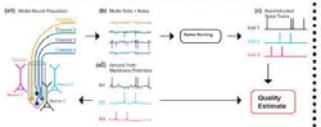

Fig. 1: Schematic of model data generation from a tetrode for testing spike sorting algorithms, taken from Einevoll et al. 2012[1].

- We model realistic extracellular activity as recorded by
  - Tetrodes
  - Polytrodes
  - Multi-electrode arrays (MEA)
- We utilize multicompartment neuron models to generate plausible extracellular spike recordings
- Test-data provided on www.g-node.org/spike

Forward modeling of LFPs

- Tools and assumptions:

LFPy nest::simulate() python

- LFPy is an integrated simulation framework built using NEURON as an extension to Python[2]
- Poisson's equation relate electric charges and potential in conductive media
- The potential from a point current source i:

$$\Phi(\vec{r},t) = \frac{I_i(t)}{4\pi\sigma_e|\vec{r}-\vec{r}_i'|}$$

- Extracellular potential (EP) calculations assume line-sources[3] for all membrane currents calculated using NEURON[2]. EPs from N-compartment neurons are obtained by integrating the point source equation[3] along each compartment i:

$$\Phi(\vec{r},t) = \sum_{i=1}^{N} \frac{I_i(t)}{4\pi\sigma_e} \int \frac{d\vec{r}_i'}{|\vec{r}-\vec{r}_i'|}$$

- Contributions from different cells are superimposed
- In case of MEAs, we deal with inhomogeneous extracellular media using Finite Element Methods.

Spike attenuation and smoothing

- Spike waveforms are position-dependent
- Area effects from different contact sizes modeled by spatial averaging
- Contact size primarily affects spike amplitude

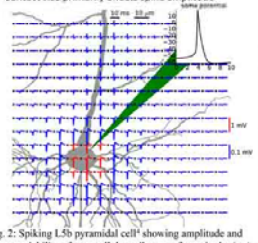

Fig. 2: Spiking L5b pyramidal cell[4] showing amplitude and shape variability of extracellular spike waveforms in the (x,z)-plane.

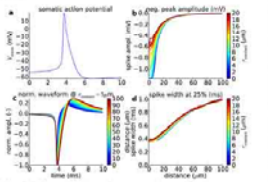

Fig. 3: Effects of electrode contact size and distance on extracellular spike. (a) Somatic action potential. (b) Negative peak amplitude. (c) Norm. spike waveform along z-axis, $r_{contact}$ = 5 µm. (d) Spike width at 25 % of peak negative amplitude.

Methods - Realistic noise

- From experimental data generate noise with
  - similar power spectral density (PSD)
  - similar frequency-dependent covariance

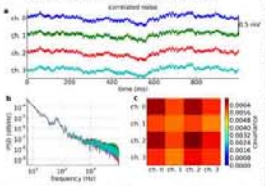

Fig 4: Artificial, correlated noise generated with PSD and covariance from experimental data. (a) Noise traces. (b) Power spectral density (PSD). (c) Channel covariance.

Methods – Spiking input

- Spiking network model employed to produce correlated synaptic events for post-synaptic model population
- Ring network topology[5], for every 4 excitatory cell we have one inhibitory cell, evenly distributed
- Feedback from extracellular noise imposed on network as non-stationary Poisson process
- Implemented in nest::[6]
- Network parameters:
  - N_E = 10k excitatory, N_I = 2.5k inhibitory
  - LIF neurons (τ_{mem} = 20 ms, V_0 = 0 mV, $\theta_{threshold}$ = 20 mV, τ_{refr} = 2 ms)
  - α-synapses (τ_s = 1 ms, τ_{delay} = 2 ms)
  - PSC amplitudes: J_E = 50 pA, J_I = $-gJ_E$, g = 6
  - Poisson noise rate: ν = 900 Hz
  - Non-stationary Poisson rate: ν = 10 Hz
  - K = 1250 nearest neighbor connectivity

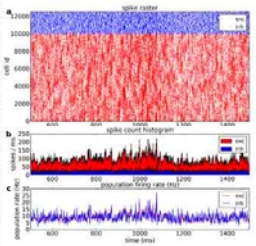

Fig. 5: Activity of spiking network. (a) Spike raster of excitatory and inhibitory populations. (b) Spike count histogram per ms. (c) Instantaneous firing rate.

Methods – Post-synaptic population

- Set up populations experimentally constrained of L5b pyramidal neurons[4]
- Synapses distributed on dendritic segments with probability normalized by surface area
- Conductance based exp2syn[7]:
  - $\tau_{rise,E}$ = 1 ms, $\tau_{decay,E}$ = 3 ms, E_E = 0 mV
  - $\tau_{rise,I}$ = 1 ms, $\tau_{decay,I}$ = 12 ms, E_I = -80 mV
  - $\omega_{synapse}$ = 0.005
- Synaptic density:
  - ρ_E = 0.025 per µm^2
  - ρ_I = 0.0125 per µm^2
- Cell IDs picked from the network simulation with Gaussian probability along the arc of the ring topology, wrapped:
  - $\sigma_E = N_E / 8$
  - $\sigma_I = N_I / 8$
  - $\rho_E = a = N_E / 8$ (postsynaptic cell n)
  - $\rho_I = a = N_I / 8$
- Ensure spike time statistics on postsynaptic cells reflect local network activity

Methods – Post-syn. pop. (cont.)

- Cells are aligned and randomly positioned in vicinity of electrode contacts and rotated arbitrarily around their z-axis
- Electrode configuration similar to sharpened tetrode (Thomas recordings, see Fig. 6 inset)

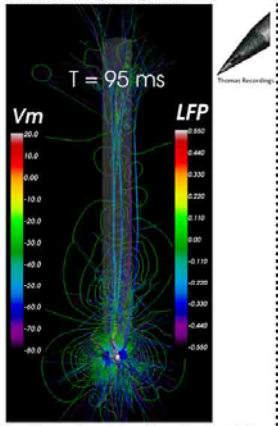

Fig. 6: Postsynaptic population with recording electrode, 8 post-synaptic L5b pyramidal cells, color coded for membrane potential. Contours display EPs in (x,z)-plane.

Results – Ground truth extraction

- The spike times used for ground truth are extracted from the somatic traces

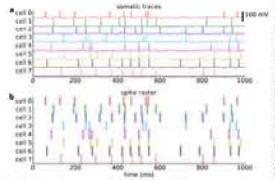

Fig. 7: Somatic traces and rasters from eight postsynaptic cells. (a) Somatic traces from the post-synaptic cells. (b) Spike raster.

Results – Test-data generation

- Extracellular potential-contributions from post-synaptic cells are superimposed
- Noise added
- Preprocessing filters applied
- Export
  - Extracellular potentials (EPs)
  - Ground truth
- Test-data uploaded to www.g-node.org/spike

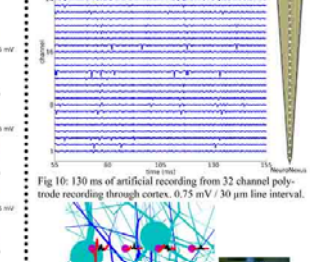

Fig. 8: Generation of test-data for testing spike-sorting algorithms. (a) Superimposed EPs from all post-synaptic cells. (b) EPs superimposed with artificial noise. (c) Multi-unit activity (300-5000 Hz, 4th order Butterworth).

- The test data can be made arbitrarily difficult in terms of overlapping spikes, signal-to-noise ratio etc.

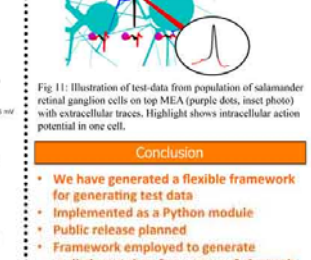

Fig. 9: Preprocessed test-data with spike templates superimposed on the trajectories. (a) 1000 ms of recording with spike templates. (b) 100 ms excerpt of (a). (c) Spike times.

Acknowledgements

- Research Council of Norway (NFR) through NevroNor, eNEURO
- INCF through the German Node
- CRCNS grant funded from NIH R01EY019965

Results - other configurations

- We have also generated test data corresponding to laminar electrodes and multi-electrode arrays:

Fig 10: 130 ms of artificial recording from 32 channel polytrode recording through cortex. 0.75 mV / 30 µm line interval.

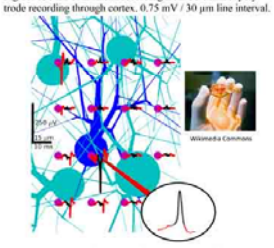

Fig 11: Illustration of test-data from population of salamander retinal ganglion cells on top MEA (purple dots, inset photo) with extracellular traces. Highlight shows intracellular action potential in one cell.

Conclusion

- We have generated a flexible framework for generating test data
- Implemented as a Python module
- Public release planned
- Framework employed to generate realistic test data for a range of electrode configurations

References

[1]Einevoll et al., *Curr Opin Neurobiol*, 22:11-17 (2012)
[2]Hines et al., *Front Neuroinformatics*, 3:1-12 (2009)
[3]Holt & Koch, *J Comput Neurosci*, 6:169-184 (1999)
[4]Hay et al., *PLoS Comput Biol*, 7:e1002107 (2011)
[5]Kriener et al., *J Comput Neurosci*, 27:177-200 (2009)
[6]Gewaltig &Diesmann, *Scholarpedia* 2(4):1430 (2007)
[7]Hendrickson et al, *J Comput Neurosci*, 30:301-321 (2011)

Example LFP from multicompartment model

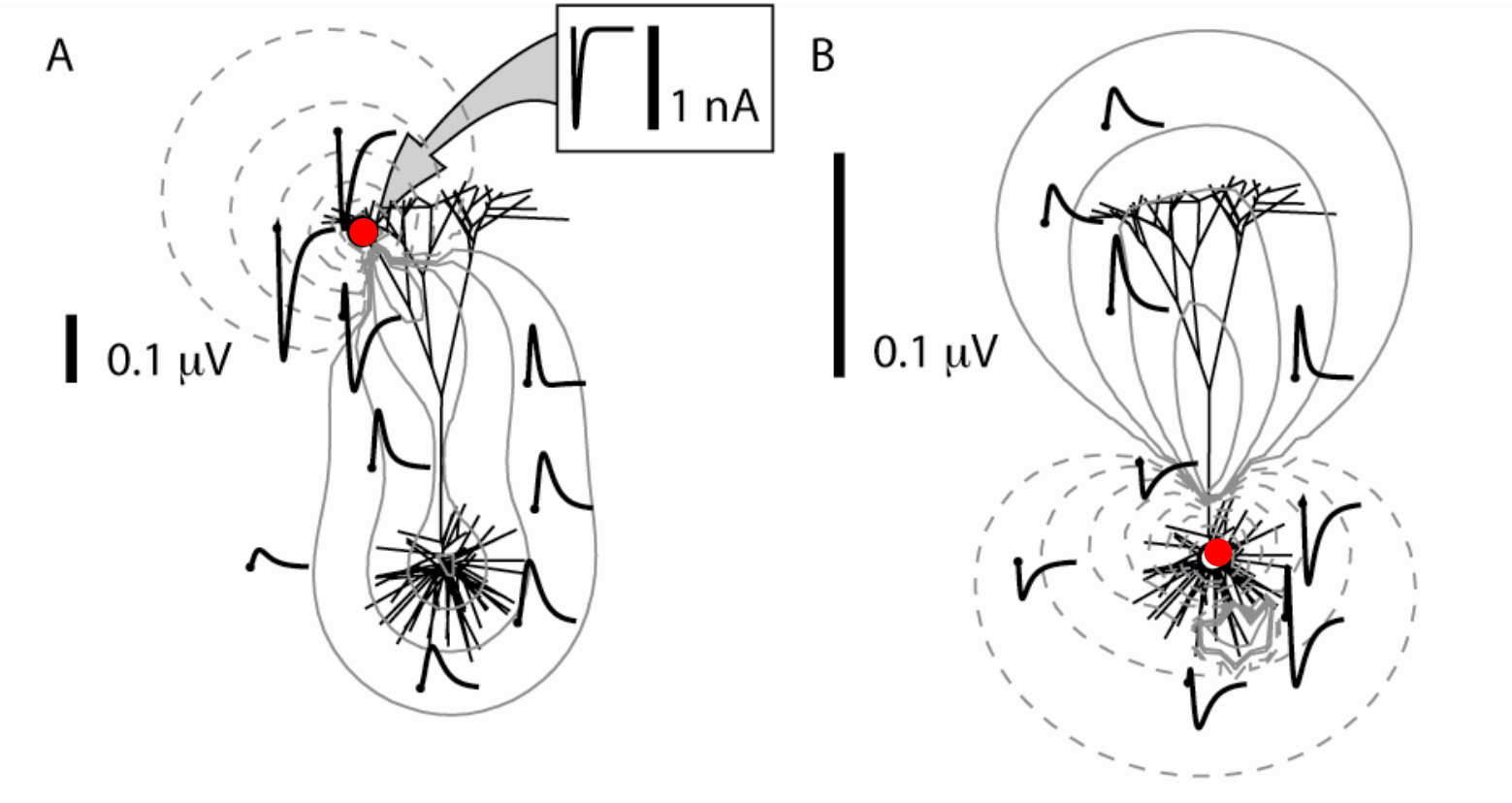

Basal excitation gives ”inverted” LFP pattern compared to apical excitation

Linden et al, Journal of Computational Neuroscience 2010

Generated LFP depend on morphology

Pyramidal
(L5 cat V1):

Stellate
(L4 cat V1):

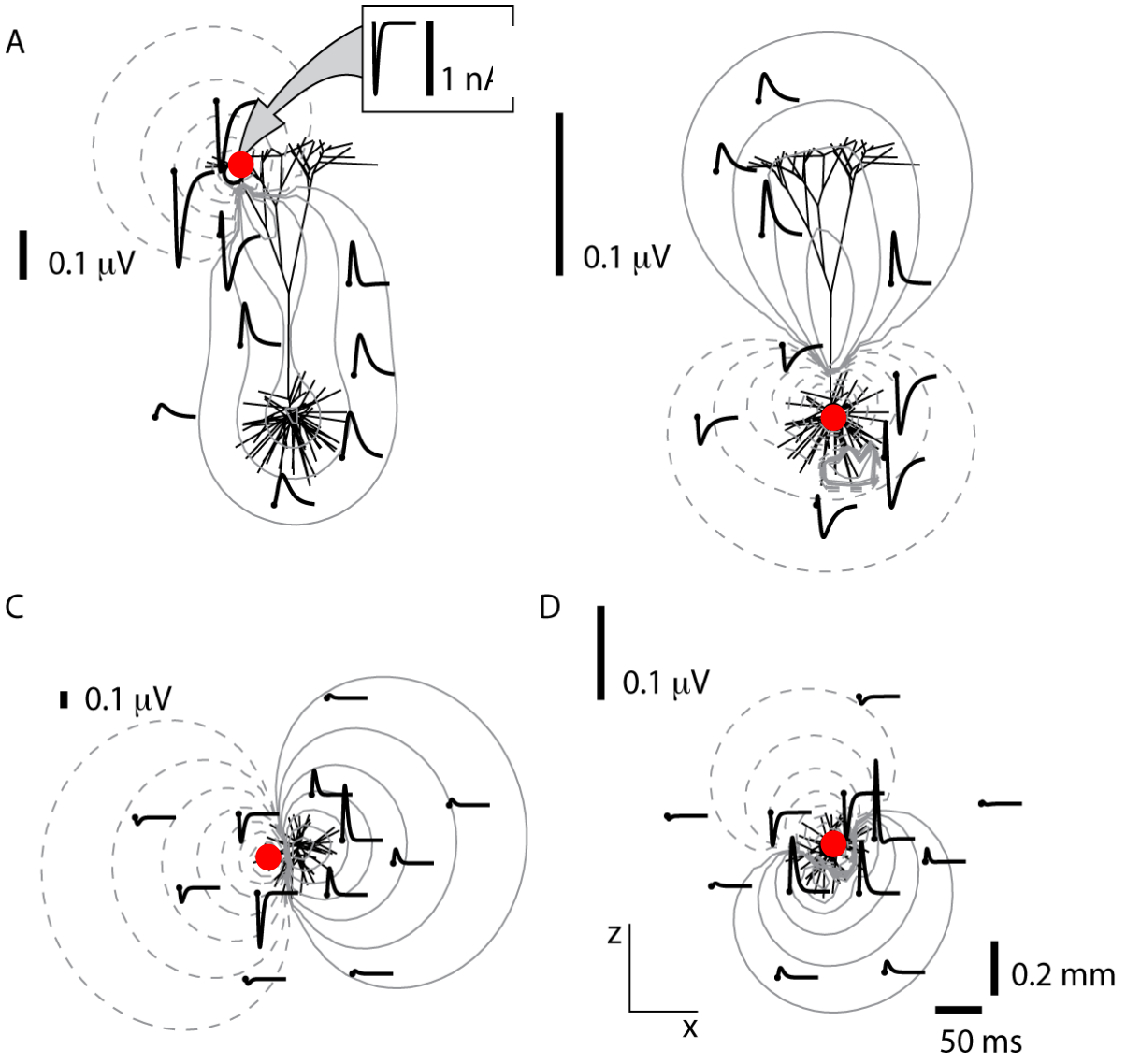

Linden et al, Journal of Computational Neuroscience 2010

LFP dipole from single L5 pyramidal neuron

1 Hz oscillatory current into apical synapse:

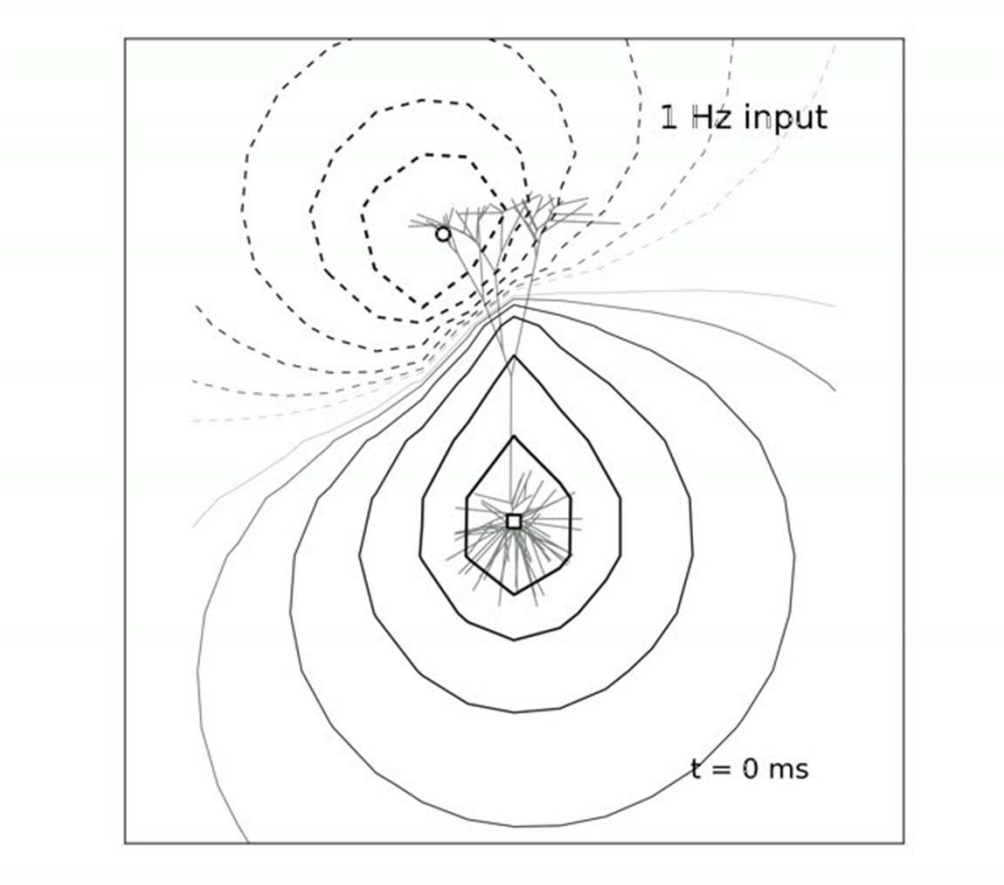

Frequency dependence of LFP dipole

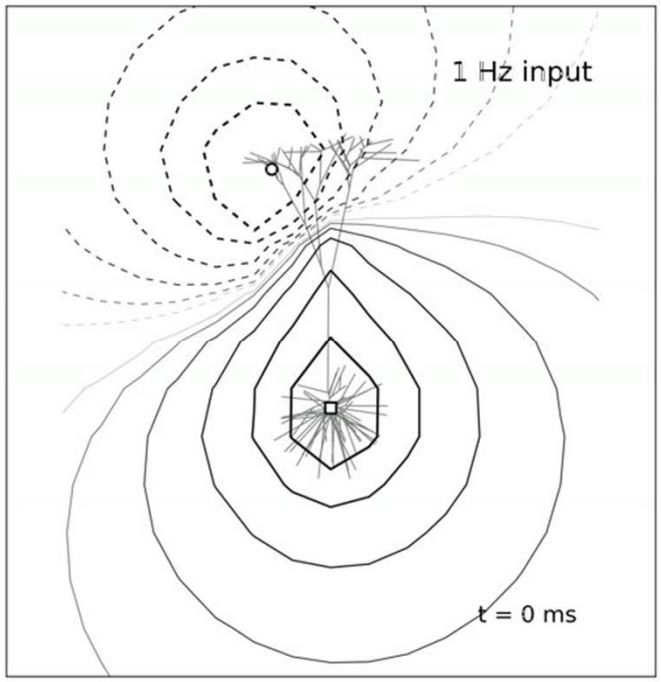

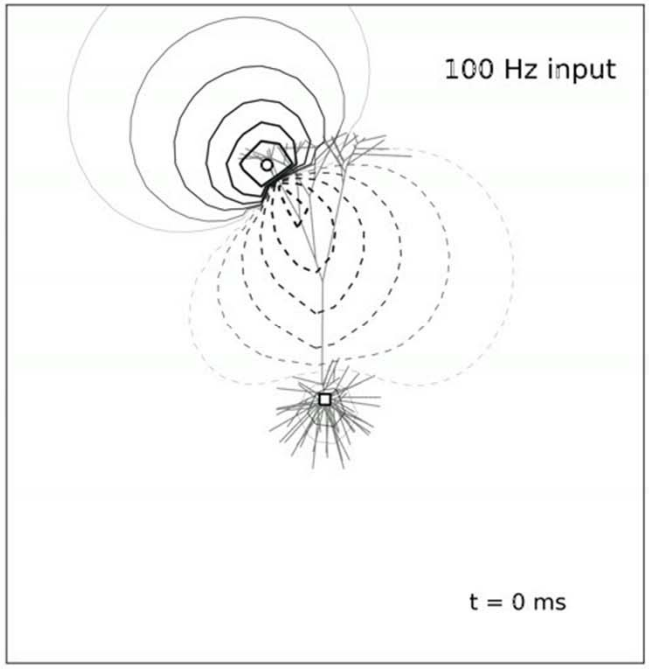

1 Hz

100 Hz

Intrinsic dendritic filtering of LFP

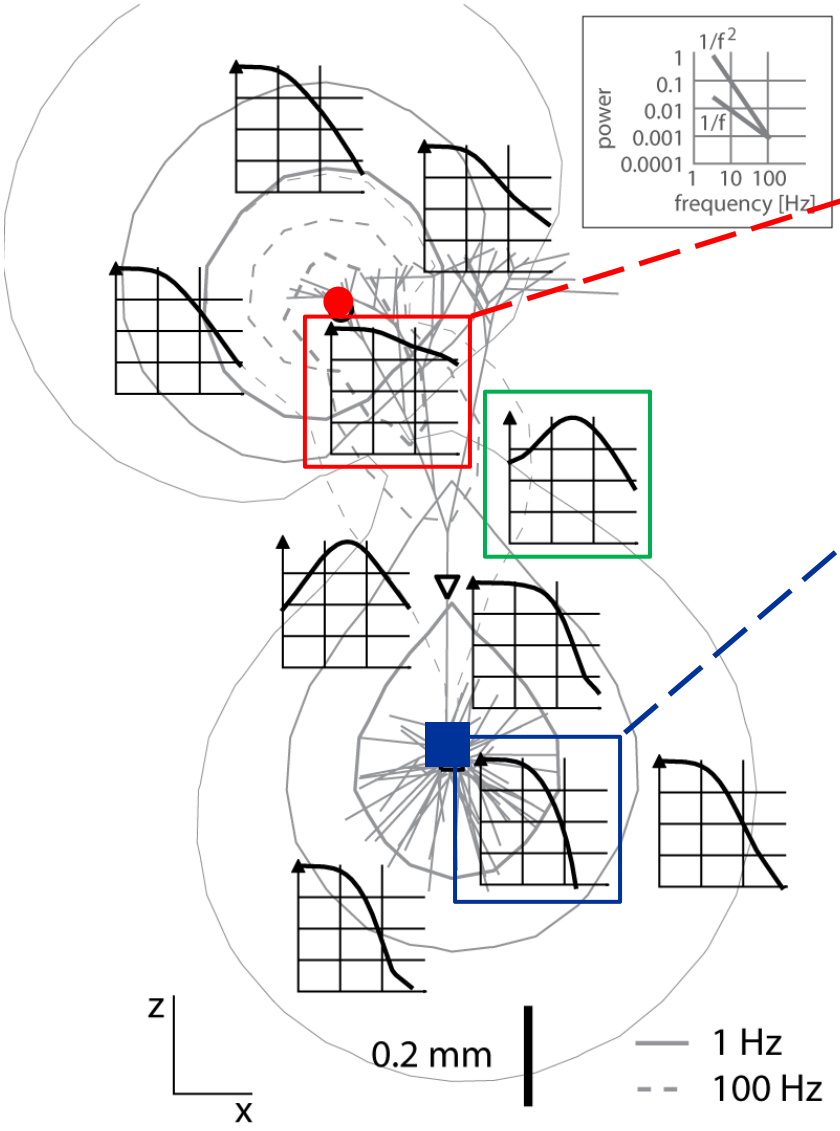

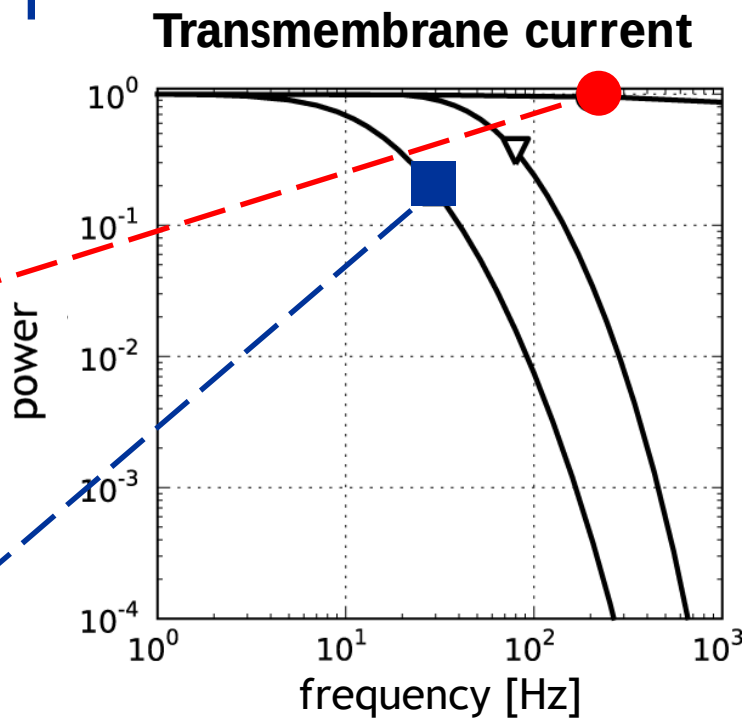

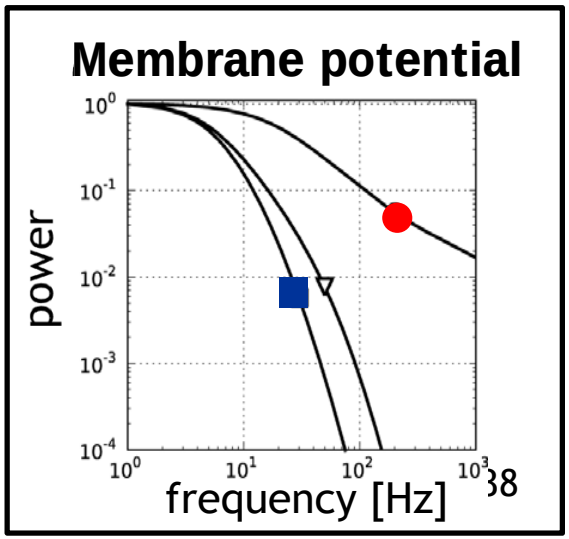

Linden et al, Journal of Computational Neuroscience 2010

Origin of low-pass filtering effect of LFP

- Depth profiles of return current:

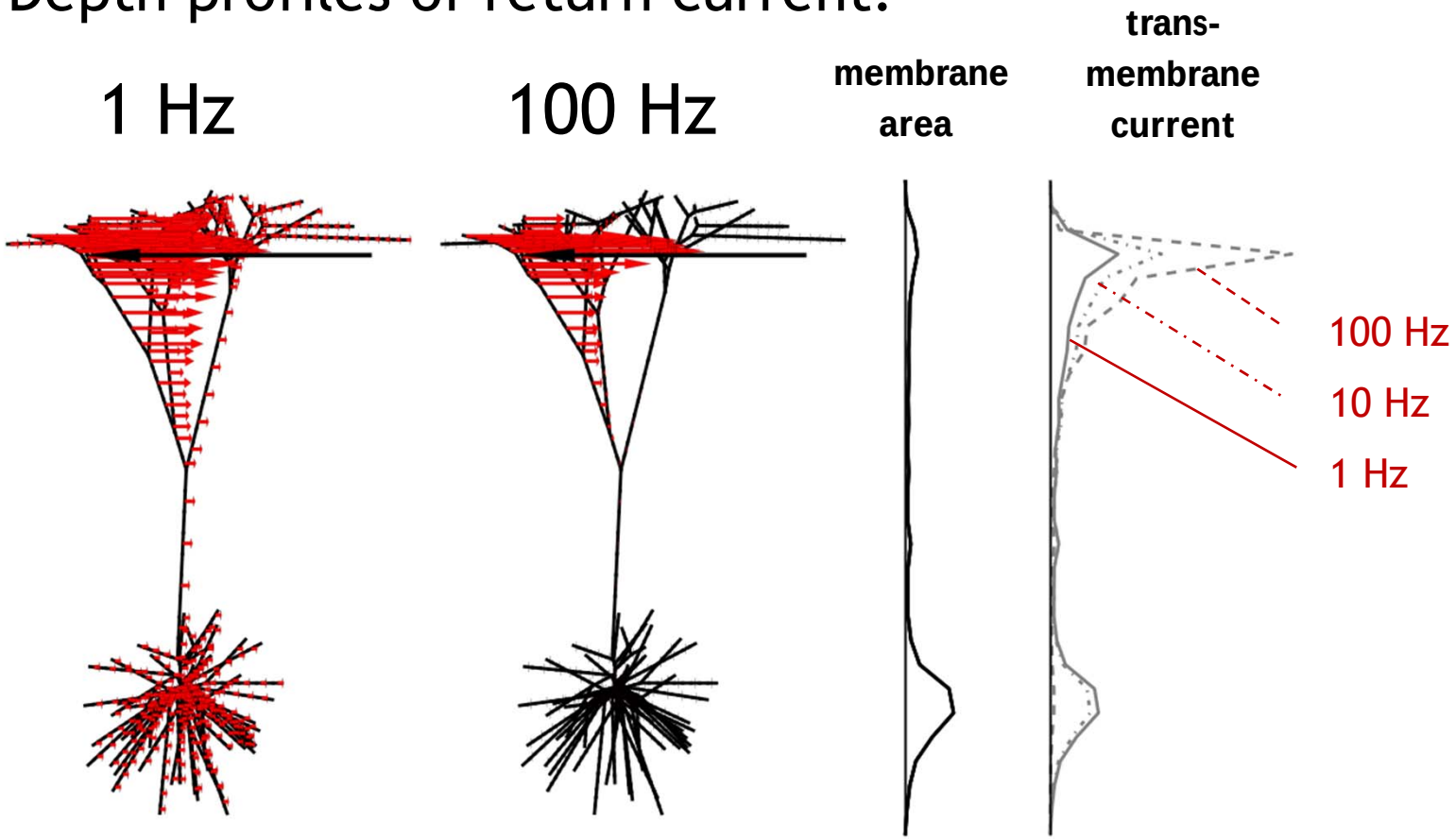

Effective current-dipole moment decreases with increasing frequency due to cable properties of dendrites

How 'local' is the local field potential?

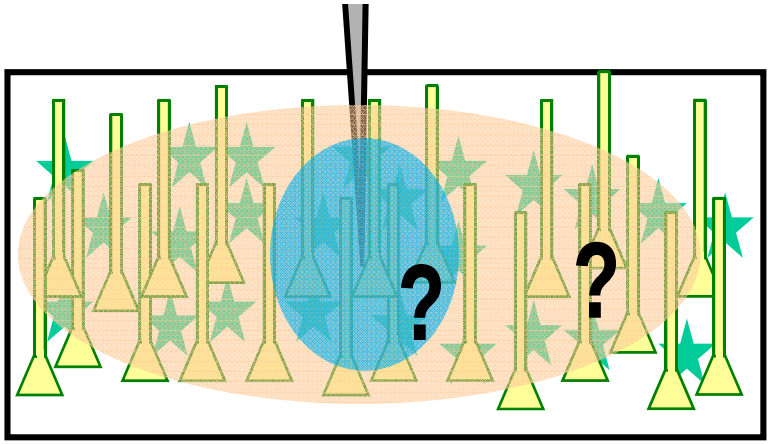

- Modeling study for **populations** of neurons:

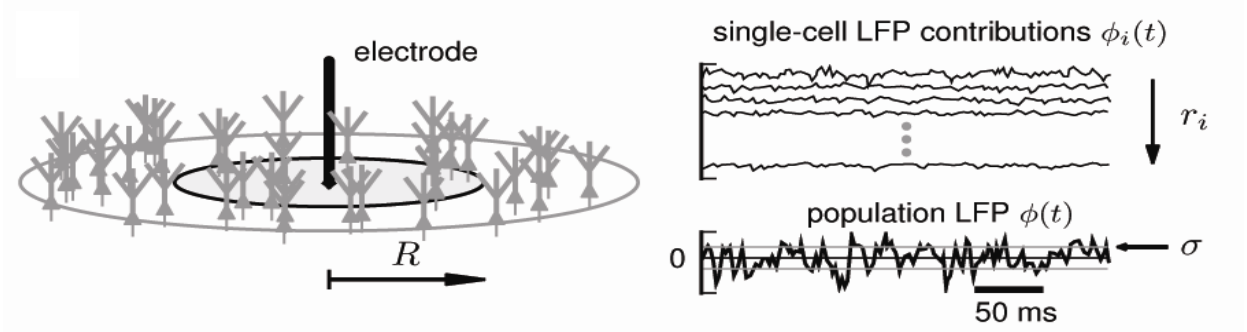

- **Uncorrelated neuronal LFP sources:** spatial reach ~ 0.2 mm

- **Correlated neuronal LFP sources:**
  - o spatial reach set by spatial range of correlations of synaptic input
  - o effect of correlations depends sensitively on synaptic input distribution

Linden et al, Neuron 2011

- **Poster on «Frequency dependence of spatial reach», Tuesday: P143**

Simplified model of the frequency dependence of the LFP's spatial reach

Szymon Łęski[1,2], Henrik Lindén[2,3], Tom Tetzlaff[2,4], Klas H. Pettersen[2], Gaute T. Einevoll[2]
[1]Nencki Institute of Experimental Biology, Warsaw, Poland [2]Norwegian University of Life Sciences, Ås, Norway
[3]Royal Institute of Technology (KTH), Stockholm, Sweden [4]Research Center Jülich, Germany
Contact: s.leski@nencki.gov.pl

Reach of the local field potential

- Cylindrical population of neurons
- Fixed radius R = 1 mm
- LFP recorded in the middle
- Which part of the population gives 95% of the LFP amplitude? (= **reach**)
- Morphologically detailed, noise-driven neurons

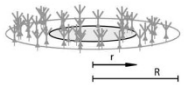

Reach depends on cell morphology, stimulation patterns, input correlations c_{in}, and also on the frequency band.

The model of population LFP

Power of population LFP:

uncorrelated contributions

$$g_0(R) = \int_0^R f(r)^2 r\,dr$$

correlated (identical) contributions

$$g_1(R) = \left(\int_0^R f(r) r\,dr\right)^2$$

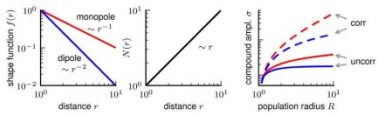

Arbitrary correlations:

$$\text{Power} = [1 - c_\Phi(\omega)]g_0(\omega, r) + c_\Phi(\omega)g_1(\omega, r)$$

c_Φ is the mean pairwise coherence between single cell's contributions

Single-cell effects

Approximation of the single-cell LFP:

- Dipole approximation far away (amplitude falls off as $1/r^2$)
- Less steep decay close to the cell (amplitude falls of as $1/\sqrt{r}$ at the soma level)
- The kink – transition to the dipole zone

Layer 5 pyramidal cell, basal input

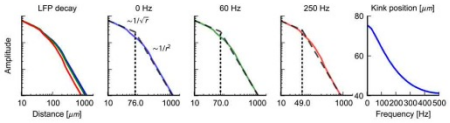

- Low-pass filtering in the dendritic tree
- The only relevant effect in a population of uncorrelated cells (power = g_0)
- In that case: reach ≈ 1.85 r_{kink}

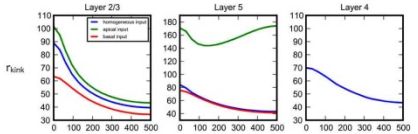

Coherence effects

Mean LFP coherence:

- Estimated from simulations
- Not flat in the frequency domain
- Direct estimation is hard, use

$$c_\Phi(\omega) = \frac{\left|\sum_{i=1}^{N} \frac{\Phi_i(\omega)}{|\Phi_i(\omega)|}\right| - N}{N(N-1)}$$

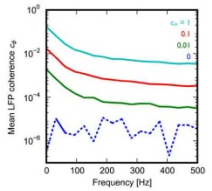

References

- H. Lindén, T. Tetzlaff, T. C. Potjans, K. H. Pettersen, S. Grün, M. Diesmann, G. T. Einevoll, Neuron 2011, 72:859–872. *Modeling the spatial reach of the LFP.*
- S. Łęski, H. Lindén, T. Tetzlaff, K. H. Pettersen, G. T. Einevoll, BMC Neuroscience 2011, 12:P88. *Spatial reach of the local field potential is frequency dependent.*
- Z. F. Mainen, T. J. Sejnowski, Nature 1996, 382:363–366. *Influence of dendritic structure on firing pattern in model neocortical neurons.*

Acknowledgements

We acknowledge support from The Research Council of Norway (eVita, NOTUR, Yggdrasil) and the Polish Ministry of Science and Higher Education (grant N N303 542839).

nencki institute of experimental biology

Simplified model predictions vs. full simulations

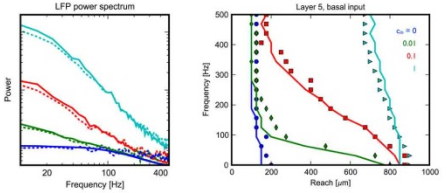

Solid: model
Dotted: full simulation

Solid: model
Markers: full simulation

Collaborators on modeling and analysis of extracellular electrical potentials

Norw. Univ. Life Sci.
- Klas Pettersen
- Espen Hagen
- Henrik Lindén (KTH)
- Tom Tetzlaff (Jülich)
- Eivind S. Norheim
- Amir Khosrowshahi
- Torbjørn Bækø Ness
- Patrick Blomquist
- Håkon Enger
- Hans E. Plesser

UC San Diego
- Anders Dale
- Anna Devor
- Eric Halgren
- Sergei Gratiy

FZ Jülich
- Markus Diesmann
- Sonja Grün

Nencki Inst, Warsaw
- Szymon Leski
- Daniel Wojcik

Hungarian Acad Sci
- Istvan Ulbert

Radboud, Nijmegen
- Dirk Schubert
- Rembrandt Bakker

ETH Zürich/Basel
- Felix Franke

TU Berlin
- Klaus Obermayer

LMU Munich (INCF G-node)
- Thomas Wachtler
- Andrey Soboloev

Funding:

Research Council of Norway (eScience, NOTUR, NevroNor)

EU (BrainScaleS)

National Institute of Health (NIH)

International Neuroinformatics Coordination Facility (INCF)

Polish-Norwegian Research Foundation

END

END OF
GAUTE